

Functions of COX-2 induced PGE₂ with special emphasis on Chick Limb Development

Agenda of this chapter

A crucial stage of embryonic development namely Organogenesis is a main focus of this section of the thesis. The extent to which the test chemical etoricoxib affected the capability of embryos to develop its organs are first described with the help of a morphological observations about differences between control and treated embryos. Later, one of the anomalies – the limb defect, was studied in-depth using the limb length determining factors and hindlimb web digesting factors. The study was extended to disease biology aspect by finding an impact of etoricoxib on dystrophic cells. For this part of study, chick embryonic skeletal muscle cells were converted to dystrophic cells, and the developed novel in-vitro model was used to study impact of COX-2 inhibition on dystrophic muscles.

INTRODUCTION

All four limbs of a single tetrapod are unique in structure. The forelimbs and hindlimbs usually carry out distinctive functions and are specialized for the same. Left and right forelimbs consisting of the same cell types, also do not have precisely the same structure as their orientation is opposite to each other. It has been a topic of exhaustive research since 1948, when Saunders described the first kind of axis in the vertebrate limb (Saunders 1948). After the most extended history of organogenetic discoveries, knowledge about limb development still remains incomplete. The research in the past two years describes how the cells of vertebrate limb sculpt the growing tissue as per a particular fate, which is almost unique to each genus (Bastida et al., 2020; Sanchez-Fernandez et al., 2020). A recent publication, for instance, describes how DNA methylation pattern differences contribute to the apoptotic fate of interdigital cells of chick hindlimb autopod (Sanchez-Fernandez et al., 2020). Bastida and co-workers defined the role of Gli3 in the thumb patterning gene modulation during chick embryonic life (Bastida et al., 2020). Most of these current research works thriving to unearth the mechanisms of human limb development, uses the chick embryo as a model organism. It has been elaborated upon how chick embryo is ideal for

organogenesis related studies earlier in the general introduction of this thesis (Chapter-1). This section deals majorly with its usefulness specifically for limb developmental studies.

Limbs of chick embryos are modified as per its mode of life i.e. walking and flying. Therefore, the anterior pair of limbs (forelimbs) are converted to the wings and the posterior pair of limbs (hindlimbs), are converted to the legs. Any aberration in the normal signalling becomes obvious due to visible differences in forelimb and hindlimb structures. In the course of development, the autopod of forelimb and that of hindlimb grows in absolutely distinct forms, which makes it easier to trace the factors necessary for each type of differentiation. Certain factors, for example SHH, FGF8, FGF10, WNT2b, etc. function for sculpting both forelimb and hindlimb simultaneously (Gilbert, 2007). However, they still do not mix the morphology of forelimb autopods while sculpting hindlimb autopods. This fact brings the upstream and downstream regulators, morphogen gradients, differential receptor possession, and many other concepts into the morphogenic picture. These developmental phenomena do not function just in case of limb development, but they also function in many other organs' genesis as well as post-embryonic development (Maden, 2020). The precise reason why studying fundamental developmental problems of embryogenesis can lead to solutions for post-embryonic issues of aging, degeneration, healing, etc is that they all comprise of common signalling pathways. Chick embryos have played significant roles in understanding embryonic development, toxicology, and disease biology while letting us know most of the current facts about these sciences (Wolpert, 2004). This work used chick as a model as well, which has been already extensively used for in-depth analyses of the limb sculpture since the 1980s (Bowen et al., 1989; Tickle, 2004).

The igniting force of limb developmental studies has been the increasing occurrence rate of the congenital anomalies such as phocomelia and amelia, which is about 10 to 40 % in various countries (Jaruratanasirikul et al., 2016). The accidents leading to appendage-loss and disease-led limb amputation also acted as fuels to those studies which reveal underlying mechanisms of regeneration of lost appendages. Statistically, about one in 190 people in USA suffers from limb loss due to innumerable reasons, while the incidence is predicted to double by the year 2050 (Ziegler-Graham et al., 2008).

Initial studies about appendage formation focussed on the environmental factors leading to limb development in metamorphosing tadpoles while they self-digest their tails. Later, after 1970 more literature was published in the area of regenerating appendages of the

Axolotls (Both, 1970). It was in the 1990s when the focus shifted to the embryogenesis of tetrapod-limbs (Vargesson, 1997). More than half a century since the proximo-distal axis mechanism was revealed, we still struggle resolving a nexus of pathways leading to precise structure of appendages. The great diversity of structure and function of limbs are generated using the same molecular players in all vertebrates. This fact forms a kind of paradox in regulation of their functions as well. The current chapter deals with identification of COX-2 as one of the participants in this process. The chapter also reveals about the organs other than limbs, which were malformed when COX-2 was inhibited.

The process of limb development in chick

In an embryonic state, limbs first appear as mere swellings on the lateral body axis on both the sides of future vertebra, then known as a primitive streak of the chick. These swellings are internally the cells which have migrated (tucked in) through the Hansen's node – an organizer of this embryo. These cells have been determined already to form appendages in the chick, in other words, their fate has been determined. The determination of this sort is carried out by those factors which are structurally mRNAs, and are derived maternally by the embryo (Ding et al., 2017). Next comes the specificity of various kinds, at least of two kinds: axes-wise and space-wise. Spatial arrangement of forelimb and hindlimb occurs via gradient-based regulation of the proteinaceous factors known as the TATA box factors (TBX) (Bamshad et al., 1997). The TBX factors work hand in hand with FGFs and WNTs to regulate which kind of limb (fore or hind) should be sculpted at a particular place. The graft cells from wing placed near the somites supposedly forming limbs in normal embryos, form limbs at the recipient site (Saunders et al., 1959). This shows importance of spatial arrangement of factors and cells both.

Development goes along the three axes of limbs simultaneously while the gradients are leading the type of limb to be formed i.e. forelimb or hindlimb, any one at a time (Towers and Tickle, 2009). Each forelimb and hindlimb consist of three axes namely proximal-distal axis, dorsal-ventral axis, and anterior-posterior axis. Proximal-distal axis refers to the shoulder-finger length in case of forelimb and the hip-toe length in case of hindlimb (figure 34). The proximal-most region is called the stylopod, middle the zeugopod and distal-most the autopod in case of both fore- and hindlimbs. The bony structures of each stylo-, zeugo-, and auto-pod are unique in forelimb and hindlimb. Forelimb is made of humerus (stylopod),

radius and ulna (zeugopod), carpals as well as metacarpals, and digits (autopod) along its grown limb length. The structures which are observed in hindlimb instead are the femur (stylopod), tibia and fibula (zeugopod), tarsus and metatarsus (autopod). These bony growths are regulated within fixed dimensions with the help of contact inhibition and cell death. The autopodal regions of hindlimb undergo programmed cell death to sculpt web-free digits. This kind of cell death also known as apoptosis is observed throughout the length of digits. Later, it gets more localized in the regions which are meant to form the joints. The apoptotic signals are suppressed in those birds which retain webbed feet ideal for their habitat such as water bodies. The molecular markers of apoptosis here like other tissues are the effector Caspases. However, the mechanism leading to heightened amount of Caspase expression is only limited to interdigital apoptotic zones, while protecting the digital regions is as interesting as the process itself (Pajni-Underwood et al., 2007).

All the described structures developed by defined mechanisms involve numerous signalling molecules active at specific time points. These molecules were found out sequentially as and when their roles in diseased conditions or congenital deformities started to be identified. Even before the function of TBX factors were known to the scientific community, COX-2 was found to be playing role in bone synthesis early in the 1990s (Forwood, 1996). However, these results were not correlated and worked upon in any separate study focussing on the action of COX-2 on bone-forming genes.

Pathways Regulating Limb Length and Web Digestion

The most common modulations arising due to developmental toxicity or abnormality are limb shortening or excessive lengthening. The reason behind this type of structural defects can be traced back to abnormal proximo-distal patterning of limbs. Patterning occurs via two main steps namely specification and differentiation of cells (Towers and Tickle, 2009). The step going on simultaneously, is cellular growth. Growth cannot be placed before or after any process in embryogenesis, as it is continuous throughout the life of an embryo. Most of the classical experiments deriving theories about the embryogenesis have been carried out in either chick or mice so far (Purushothaman et al., 2019). The limb developmental events in these two organisms are comparable in many ways. The morphological similarities and differences are as depicted in figure 34. The most obviously visible difference is of the number of digits in chick forelimb (three) and mouse forelimb (five).

From a small homogeneously populated limb bud to the variously structured autopods, plethora of processes occur at a cellular level. The cells increase in number (proliferate), grow in size and changes own shapes (differentiate), move and create a space for other cells (migrate), and probably never settle to the stability until the organism dies (Towers and Tickle, 2009). All these processes occur in the span of seven days in chick embryos, forming a limb with skeletal components from a limb bud. This process takes about five days in mice. It is relatively difficult to lay a relationship between expression pattern of genes and phenotypic characters, in such a complex process. The growth rate varies proximo-distally, being modulated by the cell cycle time disparity between regions of the same limb (Cairns, 1977). For instance, a sudden drop in amount of FGF9 (a growth-increasing factor) can not directly be related to reduction in number of cells in chick limb. It might have become more localized to smaller niche rather than being diffused in whole tissue architecture, leading to greater cell proliferation in the smaller area of its higher expression (Mariani et al., 2008). The difficulty in correlating gene expression with phenotypic variation is the major challenge while studying molecular mechanisms of limb development in models other than genetically modified organisms (Towers and Tickle, 2009) Therefore, the molecular mechanism behind the growth along proximo-distal axis of limb is still not completely understood.

One of the earliest known factors affecting cellular growth are the fibroblast growth factors (FGFs). The chick wing bud does not grow further when FGF4 and FGF8 signalling is hampered (Sun et al., 2002). FGF8 is present throughout in the length of limbs starting from the bud-formation phase till the time when skeleton is drawn. Other set of FGFs responsible for limb lengthening are – FGF4, FGF9, and FGF17. Conditional knockouts of FGF4 and FGF8 along with heterozygous activity of FGF9 led to shortening of limbs in experimental mice. These embryos possessed lesser skeletal elements than the normal embryos (Mariani et al., 2008). Other factors affecting proliferation along proximo-distal axis are GLI3 and SHH. These factors are more studied in case of regenerating limbs rather than the developing embryonic limbs. They regulate cell proliferation by directly affecting the target cells' cell-cycle completion rate (Singh et al., 2015).

Another strikingly variable characteristic of vertebrate limbs is hindlimb digit formation. While variety of land vertebrates, including humans, possess free digits in the hindlimb, number of reptiles and birds bear the webbed feet. The presence or absence of webs depend upon the mode of living of these organisms. Web is not developed selectively in

the vertebrate organisms. It is in fact present in all the embryonic forms, but are digested in later embryogenesis. In case of chick embryo, web digestion starts at day-8 of incubation and in 48-hours' time, it is completely vanished, freeing the hindlimb digits (Hamburger and Hamilton, 1951). Web digestion was initially thought to occur via necrosis, therefore, the regions undergoing cell death were called the necrotic zones in the autopod. It is now widely known to occur via programmed cell death – apoptosis. The regions of apoptosis still retain the nomenclature as ‘the necrotic zones’. The hindlimb autopodal apoptosis is brought about via inhibition of Noggin protein, which further allows BMP4 (Bone morphogenetic protein 4) to switch on the apoptotic pathway via DKK1 (*Dickkopf*) (Gilbert, 2007). The upstream regulator of Noggin is SHH, which is further regulated by FGF9. SHH has two downstream effectors, which show antagonistic effects such as cell death and proliferation. Upregulation of Noggin causes cell death and that of GLI3 causes proliferation. The decision of which pathway to be activated is strictly dependent upon spatial and temporal aspects of embryogenesis. The master regulator SHH can also elevate transcription of GREM1 (Gremlin), which shows inhibitory regulation of BMP4. The distribution of BMPs and apoptotic factors in various necrotic zones during early digestion process is depicted in figure 35 in pictorial manner.

Tightly regulated nexus of gene expression is currently not known to be affected by COX-2 derived PGs. These pathways were studied in-depth, in control and experimental embryos to find out the effect of COX-2 inhibition on overall limb development. COX-2 inhibitors are also recently been suggested as pharmacological agents to manage the condition of muscular dystrophy as they are known to function as anti-inflammatory agents. (Miyatake et al., 2016). This study was therefore extended to a disease biology from a fundamental embryology to find out, if any character of dystrophic muscles can be modified with the help of COX-2 specific inhibition other than inflammation.

Myogenesis, Muscular Dystrophy, and Dystrophic Limb Muscles in-vitro

The myogenesis pathways are crucially regulated for the normal limb development, some of which are still unknown and being researched. The main proteins participating in muscle development are Myoblast Determination Protein 1 (MYOD1), Myogenic Regulatory Factor 4 (MRF4), Myogenin (MYOG), and Myogenic factor 5 (MYF5) (Davis et al., 1987; Braun et al., 1989; Wright et al., 1989). These factors are observed in all the vertebrates being

conserved evolutionarily (Braun et al., 1989). The proper protein assembly (figure 36) as formulated after action of these myogenic factors, contains dystroglycan (α and β), sarcoglycan (α , β , and γ), and dystrophin – the protein derived from one of the longest human genes (Campbell and Kahl, 1989). The main muscle developmental defects leading to weakening of muscles usually are the results of mutation in these protein-deriving genes. Abnormal assembly of these glycoproteins lead to the abnormalities called muscular dystrophy (MD). The group of MDs are characterized by less mechanical strength of contracting muscles, poor signal transduction between myogenic cells, and simultaneously declining regenerative capacity. It is a progressive muscle weakening and atrophy, which occurs along with the heightened inflammation in the muscle niche. Owing to the multiple mechanisms of its occurrence, no particular cure has been found so far. Studies are still conducted to understand disease biology and drug inventions on models like cDMD dogs, mdx mice, and numerous cell lines (Salani et al., 2012; McGreevy et al., 2015). In the cell-lines, research is focussed on inducing dystrophy in the stem cell-derived myogenic cell lines of humans and mice. However, there are several disadvantages of such cell-line development. Firstly, there is limited ethical clearance for such studies, which follows the high failure rate of derivation of myogenic fate by stem cells after induction via extremely expensive factors (Salani et al., 2012). Other challenges involve the possibilities of genetic material being altered due to transfection methods deployed for inducing myogenesis in cells. It is equally tiresome and uneconomical to maintain these cell lines considering their insufficient numbers for cell sorting (Salani et al., 2012). In an attempt to overcome these shortcomings, researchers have explored a plethora of model organisms amongst which developing chick has been the forerunner (Intarapat and Stern, 2013). It has been extensively investigated for more than seven decades to procure a detailed understanding of the developmental aspects of myogenesis (Intarapat and Stern, 2013). It is popular amongst developmental biologists and neurobiologists for its compatibility with an array of studies involving stem cells and tissue-specific research. It is also helping a broad group of researchers studying cardiomyopathies, and other diseases like Parkinson's and MD (Ziv et al., 1994; Hutson and Kirby, 2007; Imamura et al., 2015).

In this present venture, an attempt was made to culture chick embryonic limb skeletal muscle cells and to induce MD, by blocking α -dystroglycan, a pivotal participant in dystrophin-associated sarcolemmal assembly. α -dystroglycan is a member of dystroglycan family, which is a receptor for laminin α -2, an extracellular matrix protein, mediating cell

attachment, and tissue organization (Henry and Campbell, 1999). Antibody-mediated blockade of α -dystroglycan was administered to alter the dystrophin-glycoprotein complex, eventually affecting the structural integrity of the muscle and its components.

A deliberate effort was made to block the linkage between the dystrophin and laminin α -2 in the cultured cells keeping in mind the defective glycosylation of α -dystroglycan subunit, being the proven responsible factor for human muscular dystrophy disorders (Jimenez-Mallebrera et al., 2005). Etoricoxib was added to the developed MD cell line, for identifying its effect on any molecule participating in the rescue of damaged skeletal muscle cells.

RESULTS

Morphological defects in treated embryos

The presence of COX-2 from the very first day of chick development points to its possible regulatory role in the embryogenesis. To further assess this role, the activity of COX-2 was inhibited using etoricoxib, an isotype-specific pharmacological inhibitor, and the progression of development was followed for a period of 12 days. Embryos treated with LOEC (72.2 μ g/mL) concentration of etoricoxib, showed absence of limb buds at day-2 (figure 37A) while day-4 and day-6 embryos showed gastroschisis and omphalocele (figure 37B). Haemorrhages, anophthalmia, abnormal body sizes, absence of feathers, and general developmental delay was observed in older embryos from day-8 to day-10 (figure 37C). The onset of limb development itself was delayed by the treatment with no limb buds seen in the 2-day embryos compared to the corresponding controls wherein limb buds are conspicuously visible (figure 37A). Broadly, COX-2 inhibition led to limb deformities (most commonly), followed by craniofacial and visceral deformities. The etoricoxib treatment also resulted in haemorrhage, albeit in relatively few (13%) embryos (figure 38). The most prevalent type of deformities was observed in limbs, which was therefore chosen to study further.

Morphological analysis of limb

Day-2 control and experimental embryos were stained with eosin to confirm the absence of limb bud in experimental group (figure 39). The initial observation about the length deformity was studied in depth via morphometry. The length of forelimbs did not greatly differ amongst the control and experimental groups during days 5 to 10 (figure 40 and 41). However, they were found significantly longer in day-6 treated embryos when compared to the respective control embryos. At the very same time, the hindlimbs of treated embryos were found shorter than the control embryos (figure 41). In day-8 and day-10, the hindlimbs were significantly shorter than the respective controls as well (figure 41). These results suggested a dual role of COX-2 in the regulation of limb length. The set of genes active in forelimbs caused their lengthening (at day-6), while those in hindlimb caused their shortening (at days 6, 8, and 10), when COX-2 was inhibited overall.

Hindlimb web digestion defect was then studied in the stages that experienced this phenomenon, which were days 7, 8, and 10. The web digestion process starts at day-7 in the normally developing chicks. In the control embryos of day-8, the web was partially digested, and by the end of the day 9, the digits were free, bearing no web in between. The status of web digestion in day-8 and day-10 control and experimental embryos is shown in figure 42. Web started to be resorbed at day-8 in control embryonic hindlimb autopod, while the treated embryos show minimal web resorption. At day 10, treated embryos still show presence of web at interdigital zones, in contrast to the fully digested webs and free digits of control embryos belonging to the same stage. The day-7 autopods frequently showed skeletal abnormalities in the form of excessive number of unorganized bones as observed in case of treated embryos (figure 43). This stage is the initiation point for web digestion.

Gene Expression Analysis

Treatment of etoricoxib and morphological defects were linked by analyses of limb-lengthening and web-digesting genes. Among the numerous genes checked for their presence and modulation in experimental group as compared to control, FGF9 and SHH were the only ones which were present in both forelimb and hindlimb (full length tissues) of days 6 to 10 of developing limbs. These days execute the axes development along with the lengthening of the limbs from the buds. It was found that FGF9 was upregulated in day-8 and day-10 as

compared to day-6 and day-7 of control embryos (figure 44). In the experimental group, this gene showed significant alterations in all the stages that were studied in forelimb as well as hindlimb. It decreased in day-6 as well as in day-8 forelimbs than the respective controls, while it got elevated in day-7 and day-10. This type of modulations seems to be occurring via feedback regulations rather than directional control of one gene over another. Hindlimbs of day-6 experienced the greatest up-surge of FGF9 in experimental group when compared to the control group. Day-7 experimental hindlimbs on the contrary showed lesser expression of FGF9 than the respective control group. In both day-8 and day-10, FGF9 significantly reduced than the controls.

SHH showed completely opposite trend in the forelimbs as compared to FGF9 at days 6, 8, and 10. However, at day-7, the trend reversed than other stages. Control embryos showed constantly increasing trend in SHH expression in forelimbs. In contrast to the vacillating trend of FGF9, SHH showed directional modulation (towards increasing) in all the stages in forelimb and (towards declining) in hindlimb. Hindlimb SHH dropped significantly in treated embryos as compared to the control embryos.

Genes related to web-digestion process are still not fully known, of which some are particularly pro-apoptotic present in necrotic zones, and others are present in the digits preventing apoptosis regionally. Only autopodal regions of hindlimbs were collected for this particular part of the study from day-7 (initialization of digestion), day-8 (crowing point of web digestion event), and day-10 (last phase of digestion) embryos. There was no straightforward decrease or increase in these genes, again proving the feedback-dependent regulation. FGF9 expression slightly increased in control embryos at day-10 as compared to day-8, and at day-8 than day-7. In contrast to this, the experimental hindlimb autopods highly expressed FGF9 in day-7, this level which dropped heavily at day-8, and increased a bit on day-10.

Level of GLI3 did not show significant modulation until day-10, when it declined as compared to the respective control level. It showed gradual decreasing trend in control embryos of days 7 to 10. GREM1 on the other hand showed exactly opposite pattern than that of FGF9 in the day-8 and day-10 embryos, unlike day-7, when it remained more or less similar to the respective control level. In the control embryos, GREM1 was produced less in day-8 hindlimb autopods as compared to day-7 and day-10 (figure 45A). NOG – probably the most well-known web digestion regulator showed increased expression in day-7 and day-8

hindlimb autopods as compared to their respective control embryos. The expression pattern got reversed for day-10 when it in fact dropped significantly (figure 45A).

SHH showed linear increase in control embryos while moving from day-7 to day-8, and day-10 embryos. This pattern was broken in the treated group, wherein it increased significantly than all the controls, but fluctuated among treated groups, instead of showing the gradual increase (figure 45B). There was no significant change in the pattern of SMO expression between control and treated groups. The major genes regulating web digestion event – the BMPs – showed upregulation at day-8 in treatment group as compared to control (figure 45B), which was not the case at day-7 and day-10. The experimental embryonic hindlimb autopods expressed slightly greater and lesser BMP2 and BMP7 respectively than their control levels (figure 45B). The widely known as growth-inducing factor – FGF8 got downregulated in the experimental embryos in comparison with their respective controls on day-8 and day-10 (figure 45C). TIMP3 – The factor being known as cell-migration marker and proposed as a web digestion marker, decreased in both day-8 and day-10 embryos as compared to the control levels. Finally, the ultimate marker of cell death – CASP3 was found to be increasing in treated embryos in comparison with the control embryos, which was a striking result of COX-2 inhibition (figure 45C).

Immunohistochemistry

Looking at the malformations of limb development one was interested to look upon the locations of COX-2 protein in case of various regions of forelimb and hindlimb that were checked by immunostaining of the same, in freshly collected and sectioned (using Cryostat Microtome) tissues. This experiment showed the presence of COX-2 in epithelial layer in case of autopod of hindlimb of day 8 (figure 47B). It was seen in the whole tissue in case of zeugopod of the same stage. However, COX-2 was localized more in the regions of cartilage condensation (figure 47A). Again, in forelimb it was localized in epithelial layer in autopod and in whole tissue in zeugopod (figure 46). Here, COX-2 was also seen in developing wing membrane region in both the tissue sections. In case of junction between stylopod and zeugopod, it was found to be present in the articular disc near radioulnar joint (figure 46). Overall, COX-2 was present in higher quantity in hindlimbs than in forelimbs at day-8 in the control embryos. In a more generalized perspective, COX-2 showed up in the tissues which were growing actively in the whole organ.

Caspase Localization in Web region

The embryos of control and experimental groups showed cl. Caspase3 displacement, as found out during the immunolocalization of the same. It was present at the edge of all the digits and towards distal edge of webs in control day-8 hindlimb autopods and got faded from the web edges towards the interdigital necrotic zone (figure 48A). In contrast to this, treated autopods lacked its expression on the digits, instead it was localized only in the web region of autopods, the intensity of which was lesser than that of control (figure 48B). On the contrary, cl. Caspase3 was localized on the extreme tips of digits of control autopod, as compared to the remaining web of treated autopod (figure 48C and 48D). Morphologically, the web in experimental hindlimbs showed wavy and rough margins as compared to control one on day-8 (figure 48).

chicken Embryonic Skeletal Muscle Cells (cESMC) in-vitro

The cESMC showed a typical myoblastic morphology possessing large cell bodies with numerous extensions – cellular processes. On the third day after seeding, these cells started fusing in the culture vessels and started making myotubes in-vitro (figure 49). The fused myotube clearly exhibited the presence of multiple nuclei, which are more clearly depicted with LADD staining as described later. Twelve days after the fusion was initiated, these cESMC formed multi-layered myofibres.

Induction of Dystrophy in cESMC

Muscular dystrophy was induced by addition of anti- α -dystroglycan (anti- α -DG) antibody to the cell culture media. Dystrophic condition was confirmed with the help of several assays namely trypan blue exclusion test, morphometry and contractibility assay of myotubes, cell fusion index (LADD and DAPI staining), cell death assays (EtBr/AO staining, cl.CASP3 immunocytochemistry and western blot), and dystrophic markers' (β -dystroglycan and MyoD1) immunostaining and gene expression analyses.

Trypan Blue Cell Exclusion Test

The dose concentration of anti- α -DG was decided mainly based on the extent of the resulting mortality by each of them. More than half population of the cultured cells vanished in 24

hours, when 2.1 ppb dose was administered. Rapid and intense cell death of this sort can lead to heightened inflammatory response by cells, ultimately leading to breakdown of an in-vitro system. A model for study of MD should be able to survive for longer duration. Viability increased marginally when 1.05 ppb concentration was dissolved into the culture media. After a couple of more attempts, 0.525 ppb was finalised as the treatment concentration, which caused less than 10 % mortality in the span of 24 hours (figure 50).

Morphometry

Cells were administered with 0.525 ppb anti- α -DG in the treatment (experimental) group this experiment onwards. Percentage fusion of myoblasts in control and treated cultures were as shown in figure 51A. There was significant drop in the ability of primary cESMC to fuse together and form myotubes due to anti- α -DG. The control cells exhibited higher fusion index than these treated cells (figure 51A).

Morphological features of dystrophic muscles such as wavy margins and bifurcated ends of myofibres, their breakage, and excessive damage leading to detachment of cells – were all observed in this newly developed culture (figure 52A-G). The important character of myoblasts to get arranged in a unidirectional manner was also lost in the treated culture, while the control cells grew exhibiting normal morphology (figure 52H, I).

LADD and DAPI staining

Quantification of myotubes was done using LADD staining (figure 53), making the fusion more easily observable. The multinucleated myoblasts get stained with purple blue color as opposed to pink-colored separate myoblasts in LADD stained cultures. An evident decrease in the fusing cells in treatment group as compared to the control groups can be observed in figure 53. Multinucleation is the characteristic feature of myogenic cell line, which was hampered by anti- α -DG antibody addition in these dystrophic cESMC.

Cell Death Analysis

The characteristic feature of dystrophic muscles is uncontrolled cell death leading to inability of the regenerating system to cope up with the ongoing damage. Here, the cells were stained

with EtBr/AO (ethidium bromide/acridine orange) stain to understand the difference between apoptotic status of control and treated cultures. This staining procedure enabled us to find out the extent of necrosis as well. The stage of primary myotube formation of treated culture showed both – necrosis and apoptosis (figures 54B, 54D), which was evident by the red and orange fluorescence respectively. The control cells on the contrary, predominantly showed green fluorescence (figures 54A, 54C). Statistically, about thirty percent of total cells were apoptotic as compared to less than ten percent apoptotic index of control cultures (figure 51).

Immunocytochemistry

Immunolocalization of cl. Caspase3 further represented the atrophic state in the treated cultures as compared to the control ones (figure 55). The fluorescent labelled secondary antibody (FITC-labelled) was used for detection of cl. Caspase3 in both control and treated cultures. The treated myoblasts showed intense fluorescence, when compared to control, which showed the basal level fluorescence for cESMC. Western blot was performed from the isolated proteins of both these groups, which revealed that it significantly increased in treatment culture. Alleviation of MyoD protein is one of the characters of dystrophic muscles. In the current work, the treated cells showed negligible expression of MyoD as compared to the control group. The bright field images were also captured and placed in figure 56.

Myogenic Marker Genes

Experimental cells showed the similar gene expression profile to that of the known dystrophic cells. Myogenic genes such as MYOD1, MYF5, LAMA2, and MYOG diminished significantly as compared to the control cells (figure 57A). The characteristic upregulation of TGF β was also evident in the treated cultures (figure 57A).

Effect of Etoricoxib on Dystrophic cESMC

Administration of etoricoxib to the dystrophic cESMC could deplete expression of TGF β , which is a good sign for the regenerating muscle (figure 58). However, it did not cause any improvement in dystrophic morphology, in fact, expression of MyoD protein reduced after addition of etoricoxib (figure 59). There was no particular variation in gene expression

pattern of MYF5, LAMA2, and MYOG in etoricoxib treated embryos as compared to anti- α -DG treated cultures (figure 57B). This proves that COX-2 might be acting on non-muscle cells, stimulating them to release some myogenic factors, in case of muscle regeneration. In this scenario, the culture lacked any other type of cells, which probably led to the stability of these genes' expression.

DISCUSSION

Vertebrate limb development is a vast area of research involving a plethora of molecules having been identified by research gradually in all these years. The three most used model organisms for limb developmental studies are chick embryos, mice, and adult salamanders (Purushothaman et al., 2019). Even though the mice are closer to humans, chicks share considerable similarity of molecular aspects with humans (Hillier et al., 2014). Some of the known facts of annexed molecular pathways sculpting the complex limbs from relatively smaller pool of homogenous cell population – the mesenchyme, have been derived from the regenerating systems as well. Process of limb development is not just researched by developmental biologists, but is also of keen interest to the evolutionary biologists, embryologists, pathologists, and system biologists. Numerous molecules involved in the limb generating pathways have been identified now, and the research is more focussed on how these factors are connected to each other (Zuniga, 2015). The current work however, proposes the new molecule participating in the embryonic development of the limbs, which is COX-2. It has long been associated with regenerating system by other researchers of our lab, wherein its inhibition delayed the course of wound healing via interaction to MMP, WNTs, and FGFs (Buch et al., 2018). In this study, we found that structurally, COX-2 inhibition led to defects of multiple types. Some embryos lacked eyes, while the other had developed abnormal craniofacial features. However, the most frequent abnormalities were related to limbs. Some of the embryos possessed shorter limbs, while the others had undigested webs (syndactyly – partial or complete) on day-10 of incubation.

FGFs are known to be affecting all the events of embryogenesis involving cellular growth. The particular types of FGFs involved in limb development are FGF4, FGF9, FGF17, FGF8, and FGF10, of which, FGF8 and FGF10 maintain the proliferative state in the mesenchymal niche of developing limb-bud (Purushothaman et al., 2019). In this work, the

level of FGF9 dropped in hindlimbs of day-8 and day-9, which coincided with the decreased limb lengths of the same samples (figure 41 and 44). Levels of SHH declined to more extent than that of FGF9 in both these samples (day-8 and day-9 hindlimbs) (figure 44). This proved the possible function of COX-2 in regulation of FGF9 and SHH in the normal tissues, because they got downregulated when COX-2 was selectively inhibited causing the phenotypic shortening of limbs at the same stages. The treated forelimbs grew longer than the control forelimbs of day-6 embryos (figure 41A). At this timepoint, the rise in forelimb length coincided with SHH upregulation in the same (figure 44), showing the direct effect of SHH on limb lengthening, as affected by Etoricoxib addition. The same limbs showed lower concentrations of FGF9, which differed from pattern of SHH and phenotypic length of limbs. Overall, it was proven that COX-2 has dual effects on FGF9 and/or SHH expression pattern, which can be upregulated or downregulated based on concentration, space, and time – dependent manner. Ultimately, in the present study, COX-2 was found to affect limb length via modulation in FGF9 and SHH expression patterns.

Regarding the presence of web in hindlimb autopods, it was found that FGF9 was significantly upregulated in the etoricoxib treated embryos (figure 45). However, FGF9 level declined in the whole hindlimb tissue as compared to control (figure 44). This comparison made it obvious that rather than expression levels, the localizations changed for FGF9, and probably number of other factors, which was not in the scope of this research to evaluate. Nonetheless, this work points out the displacement of apoptotic factor cleaved Caspase3 in case of hindlimb autopod, which was studied with the help of immunolocalization of the cl. Caspase3 in 8 and 10 days hindlimb autopods of control and treated groups. This kind of effect might be having the displacement of upstream factors of cl. Caspase3 as well. Caspase3 is activated at necrotic zones by the effect of several upstream factors such as BMP2 and BMP7. This study revealed that the level of BMPs did not differ in control and treated tissues in early stage of web digestion initiation (day-7) (figure 45B). However, both these significantly surged higher on day-8, which was the period of high apoptotic activity for web digestion process. Literature suggests that rather than upregulation of BMPs, the downregulation of FGF8 act as main trigger for interdigital cell death in limbs (Hernandez-Martinez et al., 2009). However, control autopods did not show decreased level of FGF8 in autopod of day-8 chick embryos, as compared to that of day-7 (figure 45C). It was speculated that FGF8 did not decrease in the control embryos as well, owing to their requirement in the autopodal digits, which needs to be prevented from activation of apoptosis. The specific

sampling of only webs and only digits of chick embryos was not appropriate due to the plausible manual errors which could modulate the results based on the separation of web from digits. More sophisticated techniques such as fluorescent in-situ hybridization can probably solve the issue by understanding localized levels of these genes.

Web digestion process has generated number of contradictory ideas regarding its progression and molecular details. At the molecular level, SHH was thought to regulate FGF signalling in case of hindlimb autopods at the time of web digestion in the view of a group of researchers (Purushothaman et al., 2019). However, other researchers place SHH under FGF regulation for the same process of web digestion (Crossley et al., 1996; Lewandoski et al., 2000). The event of web digestion was speculated to be necrotic in early studies (Saunders, 1966). Saunders described the process of web digestion occurring via phagocytosis, as a massive cell death event (Saunders, 1966). The understanding has now been changed, suggesting web digestion as a progressive cell death (Hernandez-Martinez et al., 2009). The ideas about functioning of pathways keep changing time to time when it comes to limb development, especially during autopodal sculpture. The results of current work supported the presence of feedback loops between GREM, FGF, BMP, WNT, and SHH for regulating limb development (Jin et al., 2019).

Overall, the abnormal expression of many genes was triggered by COX-2 inhibition in the limbs of developing chicks. Some of these, such as FGF8, FGF9 and SHH – also function in axes development of all the organs of the vertebrate body (Purushothaman et al., 2019). Thus, abrupt expression of these genes could have been one of the reasons behind the kind of deformities observed in the treated embryos. The organs showing abnormal morphologies could be selectively studied in future, to unearth the underlying mechanisms of action of COX-2. This study provides a glimpse of plausible action of COX-2, which has vast scope of evaluation regarding the placement of all the studied genes in the active pathways with respect to COX-2. For example, some of those genes could be strictly downstream of COX-2, and others could change their places (downstream or upstream), based on the feedback regulation. The nature of regulation of these factors via COX-2 expression during embryogenesis needs further in-depth study.

The other aspect of this work was to find out the effect of etoricoxib on dystrophic limbs. The dystrophic limb muscles are characterized with prolonged inflammation, which hampers regeneration and repair in the damaged regions (Cappellari et al., 2020). COX-2

inhibitors such as etoricoxib can reduce inflammation, and thus are proposed as the drugs for treating muscular dystrophy (Miyatake et al., 2016). The first step to understand the effect of COX-2 inhibitor etoricoxib in the dystrophic condition was to develop an in-vitro model for doing so. In this particular work, the dystrophic characteristics were induced in the cultured chicken embryonic skeletal muscle cells (cESMC) isolated from 11-day old chick embryos. The decided stage was standardized after several attempts of isolating cells from days 8 to 12. Relatively less fibroblasts and more myoblasts were procured from the decided stage day-11. The cells from day-11 were less labile to the treatment and attached tightly to the surfaces allowing easy handling, as compared to other stages. The feather follicles hindered the prolonged contamination-free culture of cells isolated from day-12. The cultured cells added with anti- α -DG antibody (IIH6, DSHB, USA). The similar approach was used for culture myogenic cells, which however, possessed some variations than the human cells' dystrophic characters (Brown et al., 1999). The major drawback of the most used animal model mdx mice as well as mice myogenic cultures is upregulation of utrophin protein as opposed to decreasing levels of dystrophin, which ultimately leads to less severity of disease progression as compared to humans (McGreevy et al., 2015). The currently developed model firstly acts as inexpensive and easy-to-maintain culture system. Secondly, it involves the least ethical concerns when compared to mice and human muscle cell lines. It is useful in the studies attempting to understand the fundamental characteristics of dystrophic muscle other than for primary drug evaluation. The etoricoxib added to the cells showed almost no effect on gene expression pattern of dystrophic genes namely MYF5, LAMA2, and MYOG, but it dropped level of MYOD. It was proven that etoricoxib does not work to rescue the dystrophic gene derangements. The short-term inflammation post-injury plays an essential role in healing of damages in muscles (Cappellari et al., 2020). Therefore, this work suggests that etoricoxib, or other COX-2 inhibitors should be verified for the timepoint of administration in each patient while attempting to manage the dystrophic condition. In case of otherwise, damage can elevate due to suppression of essential inflammation.

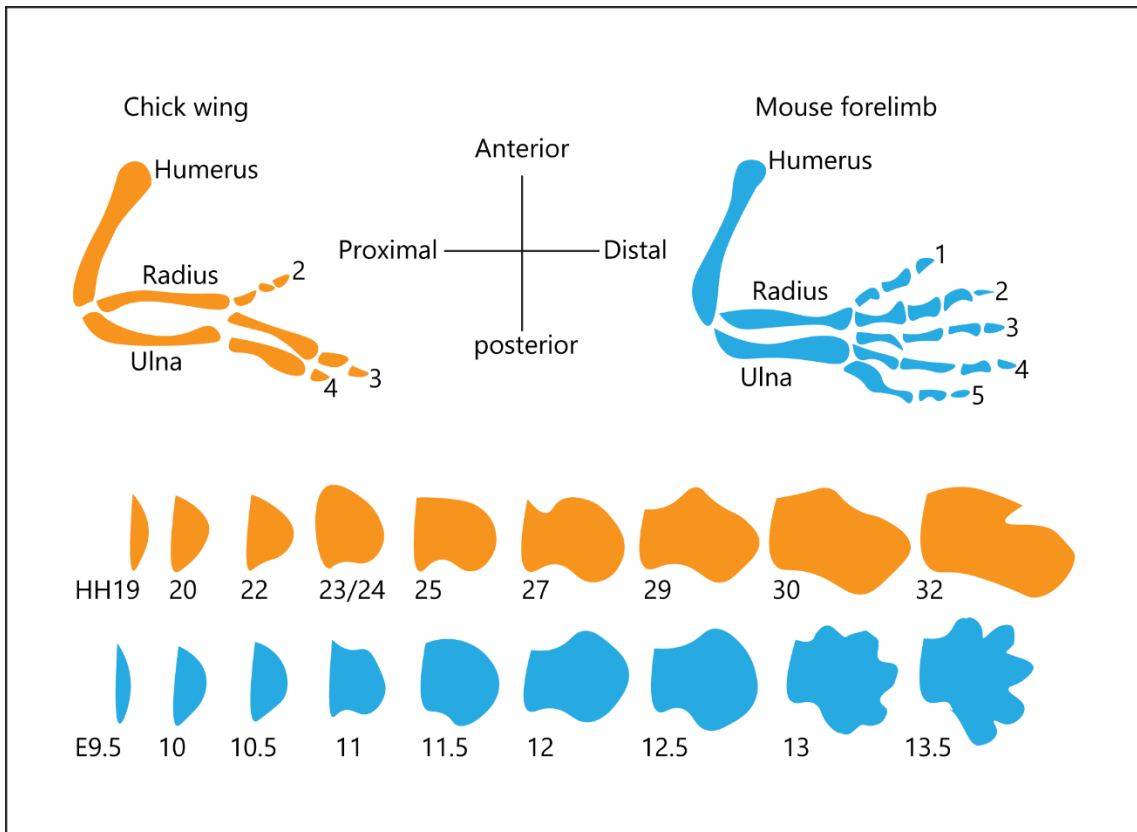


Figure 34: Chick limb components and development compared with those of mouse. The nomenclature of proximal parts of limbs – stylopod as humerus, radius and ulna as zeugopod – is same for both these. Chick forelimb autopod gets transformed to make a wing, in the process it loses the first digit and contains only three digits finally. Mouse forelimb develops web-free digits, five in number. The stages of development are also compared for differentiation process.

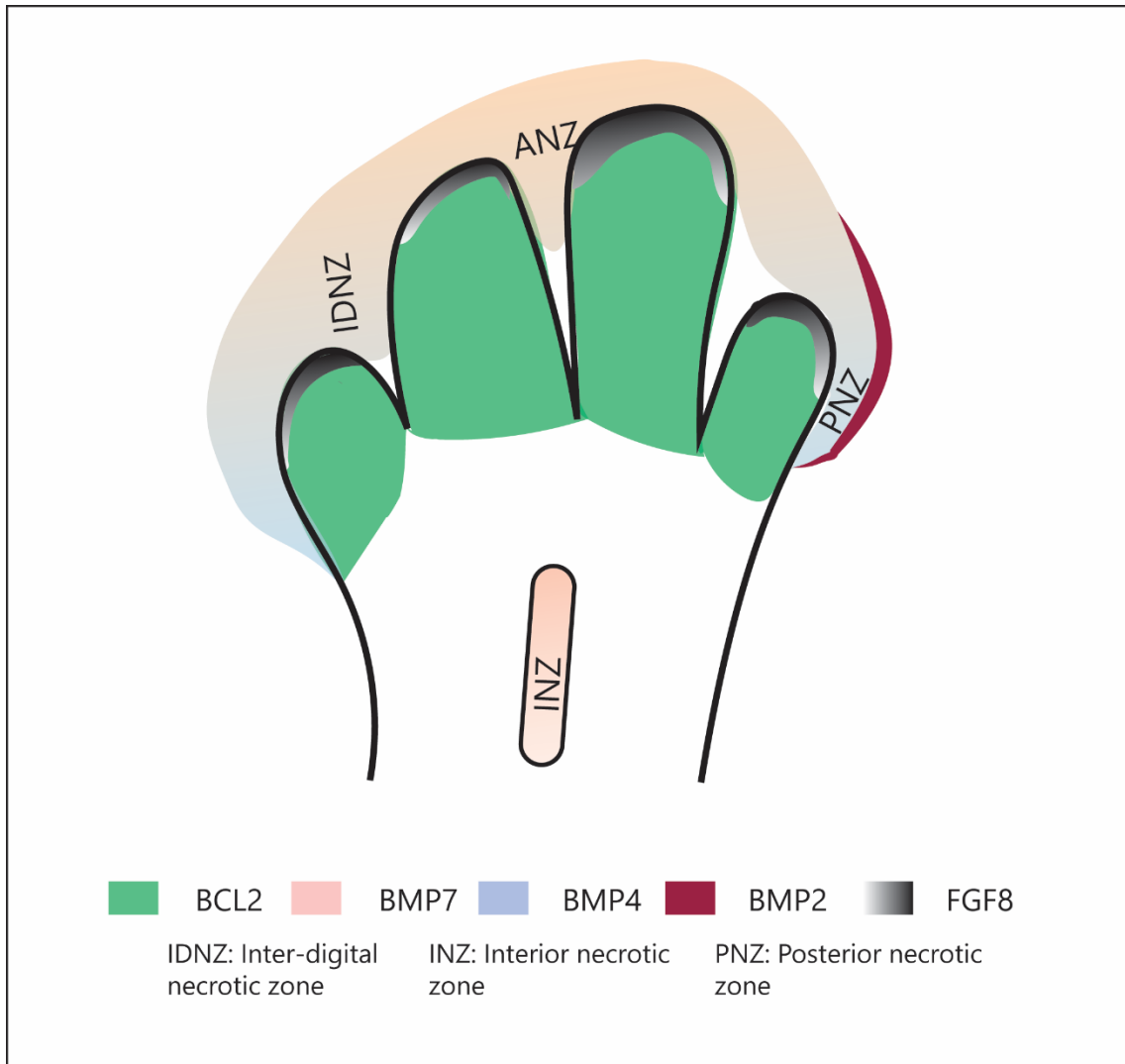


Figure 35: The necrotic zones and distribution of web-digesting factors in chick embryonic hindlimb autopod. BMP7 and BMP4 are expressed in the inter-digital necrotic zone and all over the web to be digested. BCL2 – an anti-apoptotic factor is present in the digits to be prevented from cell death. Interior necrotic zone – a region between the bones show the presence of BMP7. The anterior-most and posterior-most ends of web contain BMP4. The posterior end also express BMP2.

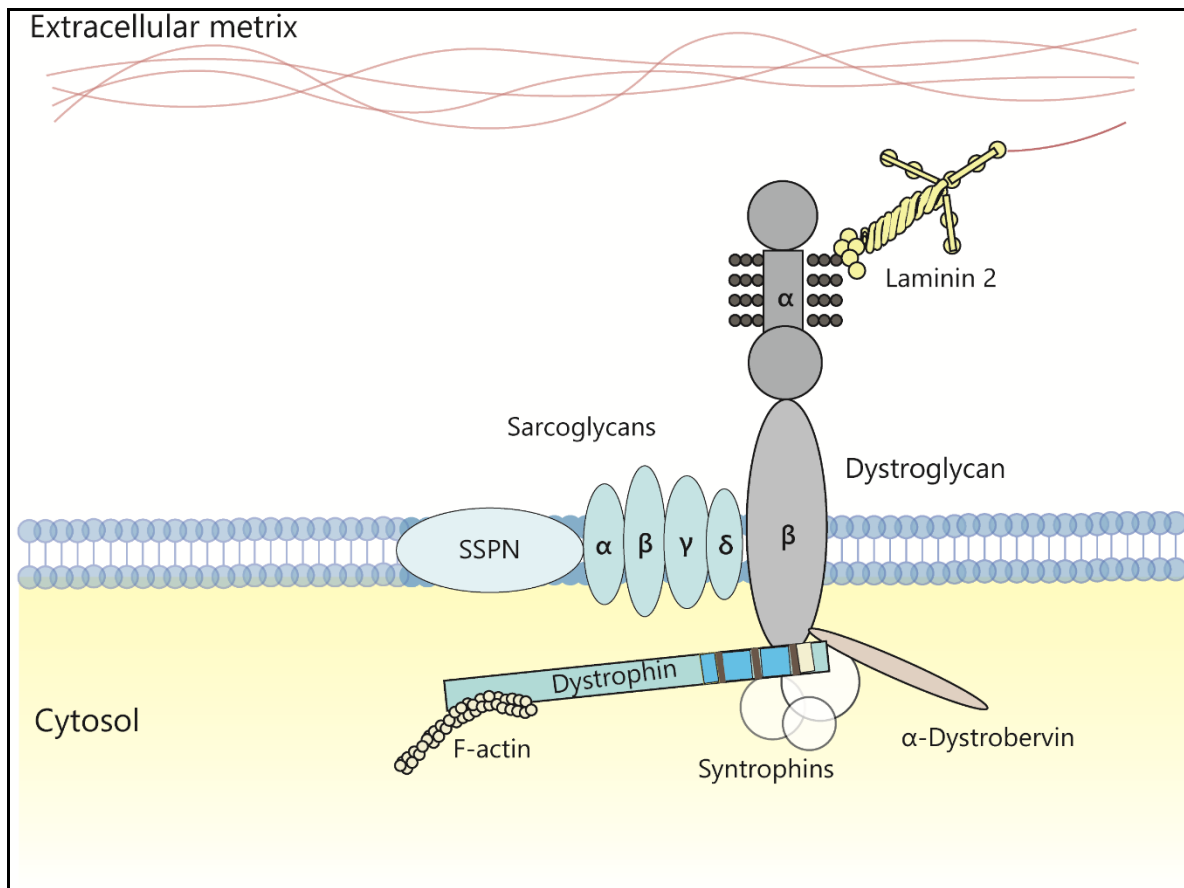


Figure 36: The sarcoplasmic assembly of dystrophin and associated proteins. Dystrophin connects the whole assembly to the cytoplasmic actin component. Laminin attaches the assembly to the extracellular matrix on the outer side of the cells. Dystroglycan mediates the interaction of whole assembly and connects it to sarcoplasm.

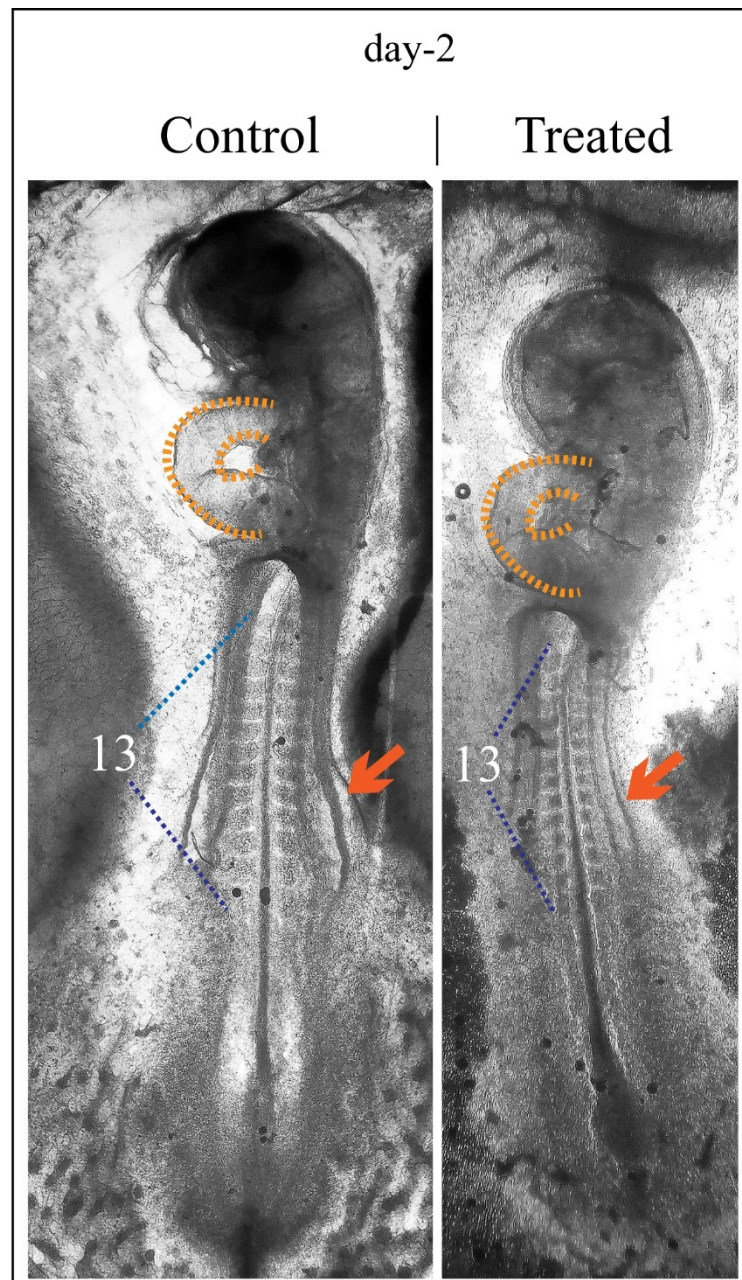


Figure 37A: Comparison of morphological features between 2-day old chick embryos of control and treated group. Absence of limb bud is marked in the treated embryo as compared to control (shown with the help of red arrows). The looped heart located on one side of the embryo rather than in center (orange dotted lines), and number of somites (13) remained similar in control and treated embryos, proving that they were isolated at the same timepoints.

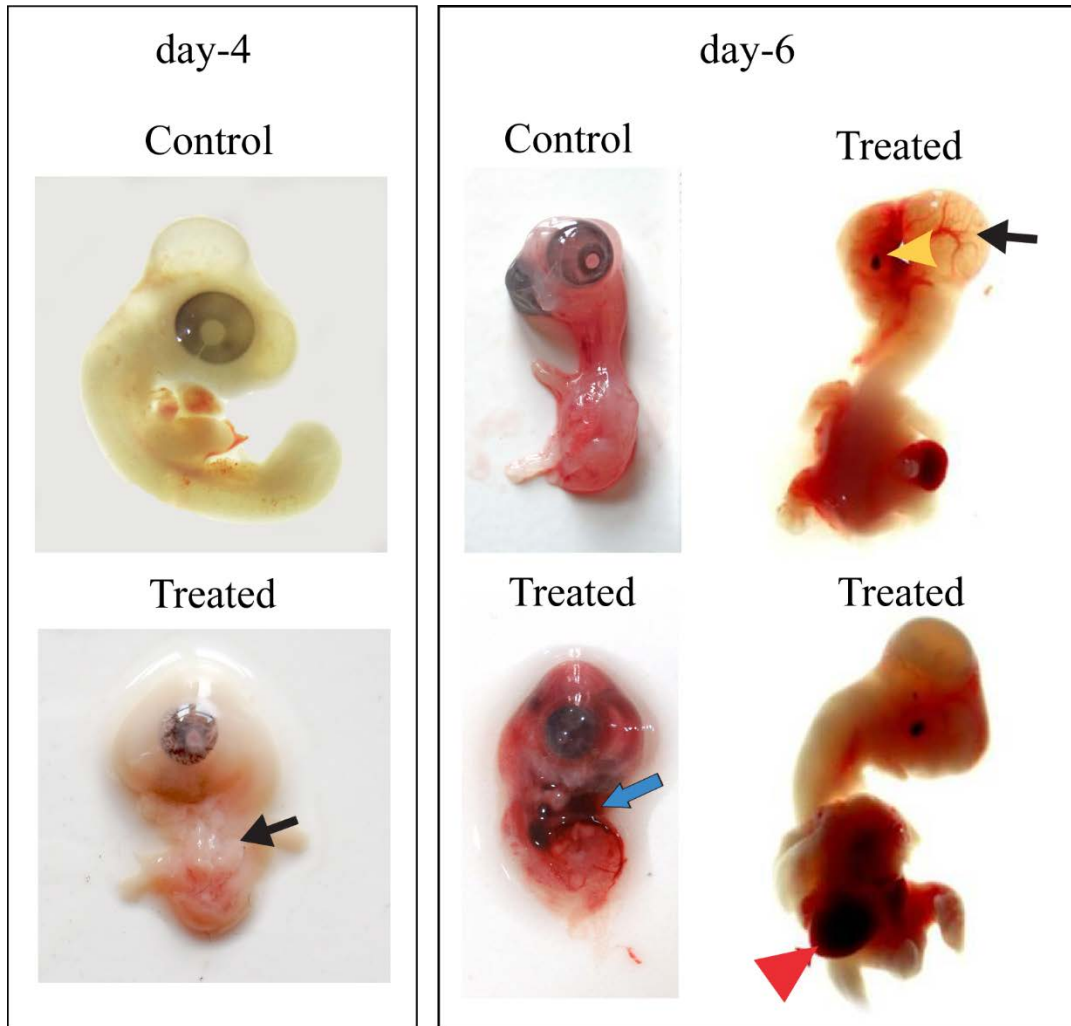


Figure 37B: Comparison of morphological features between 4- and 6-days old chick embryos of control and treated group. Day-4 treated embryos showed open ventral body wall markedly different (black arrow) than the control embryo with no viscera visible outside the body other than heart. The treated day-6 embryos showed absence of limbs (blue arrow) and larger heart (red arrow-head) when compared to the control embryo. The eye pigment, which normally develops on day-4 (as visible in day-4 control) was partially developed in day-6 treated embryo (yellow arrow-head).

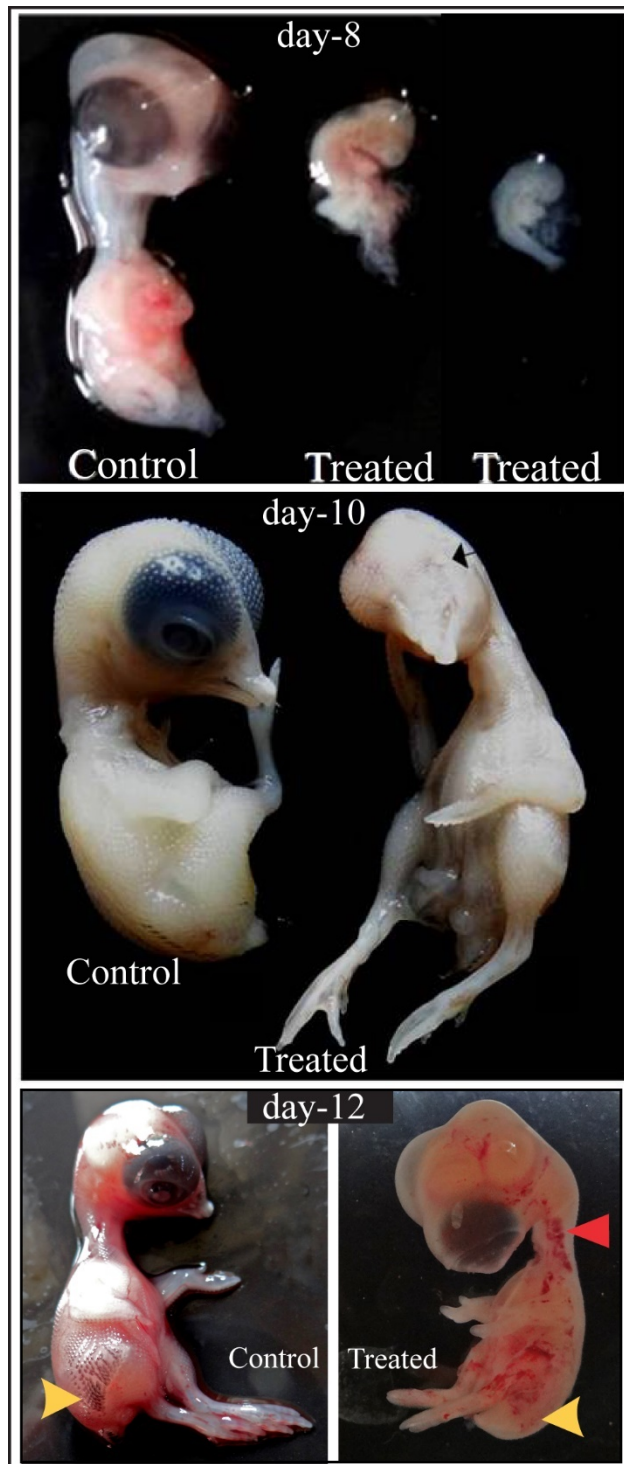


Figure 37C: Comparison of morphological features between 8, 10, and 12 days old chick embryos of control and treated group. Overall delayed development of day-8, absence of eye in day-10 treated embryo (black arrow), multiple haemorrhages in day-12 treated embryos (red arrow-head) along with absence of feathers on lateral body line (yellow arrowhead) – were the observable anomalies.

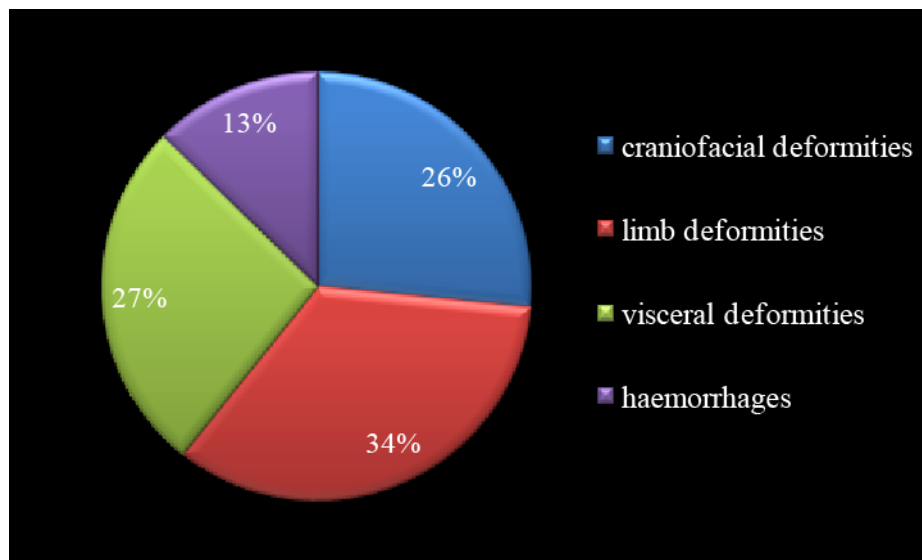


Figure 38: The frequency rate of various observed deformities in treated embryos as compared to control embryos. Highest caused anomalies were related to limb development out of the four. These included larger or shorter limbs, absence of limbs (phocomelia), and web digestion defects in hindlimbs. Next were the visceral and craniofacial deformities, including ventral body wall defects. These included omphalocele and gastroschisis. Craniofacial defects covered any morphological deviation in the head, eye, beak, and other facial features in the treatment group when compared to control. Haemorrhages occurred in a smaller number of embryos; however, was severe in the affected embryos.

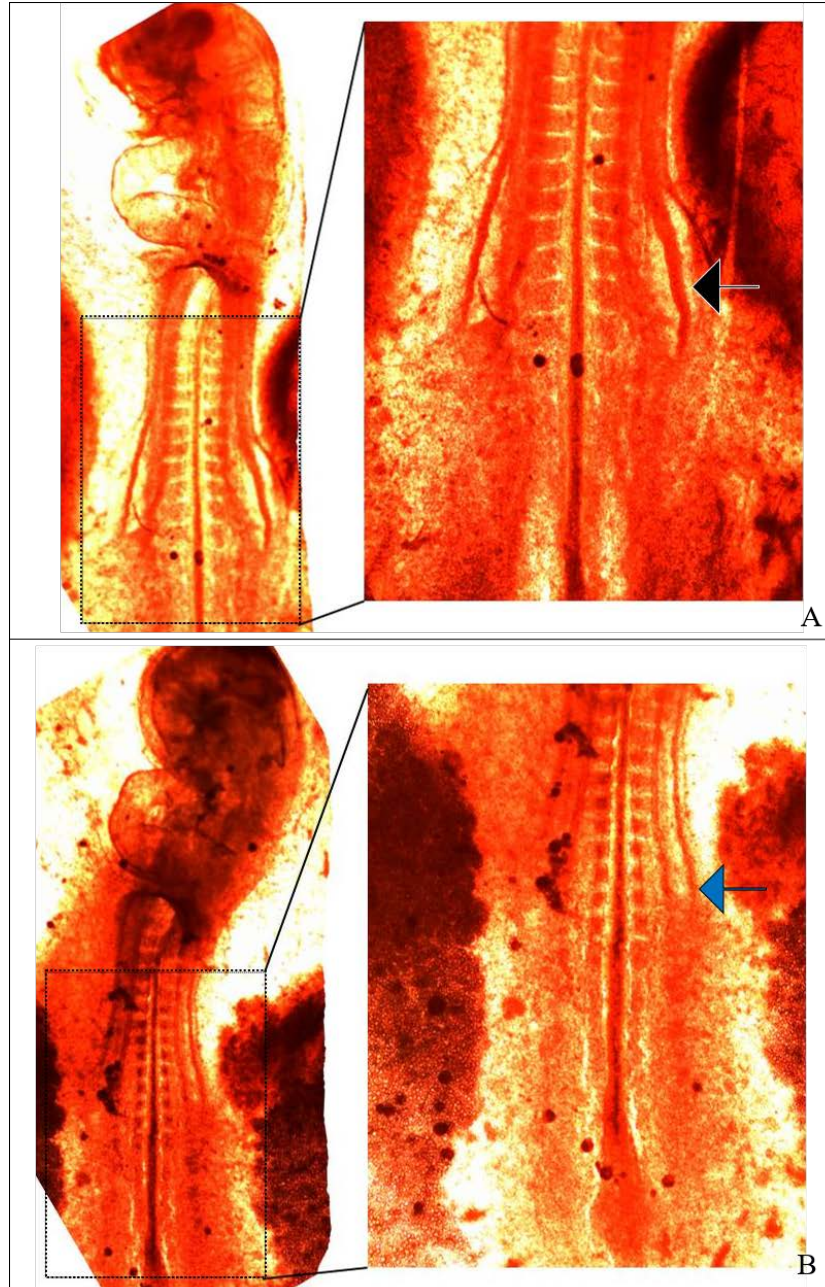


Figure 39: Absence of limb buds (blue arrow) as confirmed by eosin staining of day-2 control and treated embryos. It was conspicuously present in the treated control embryo (black arrow).

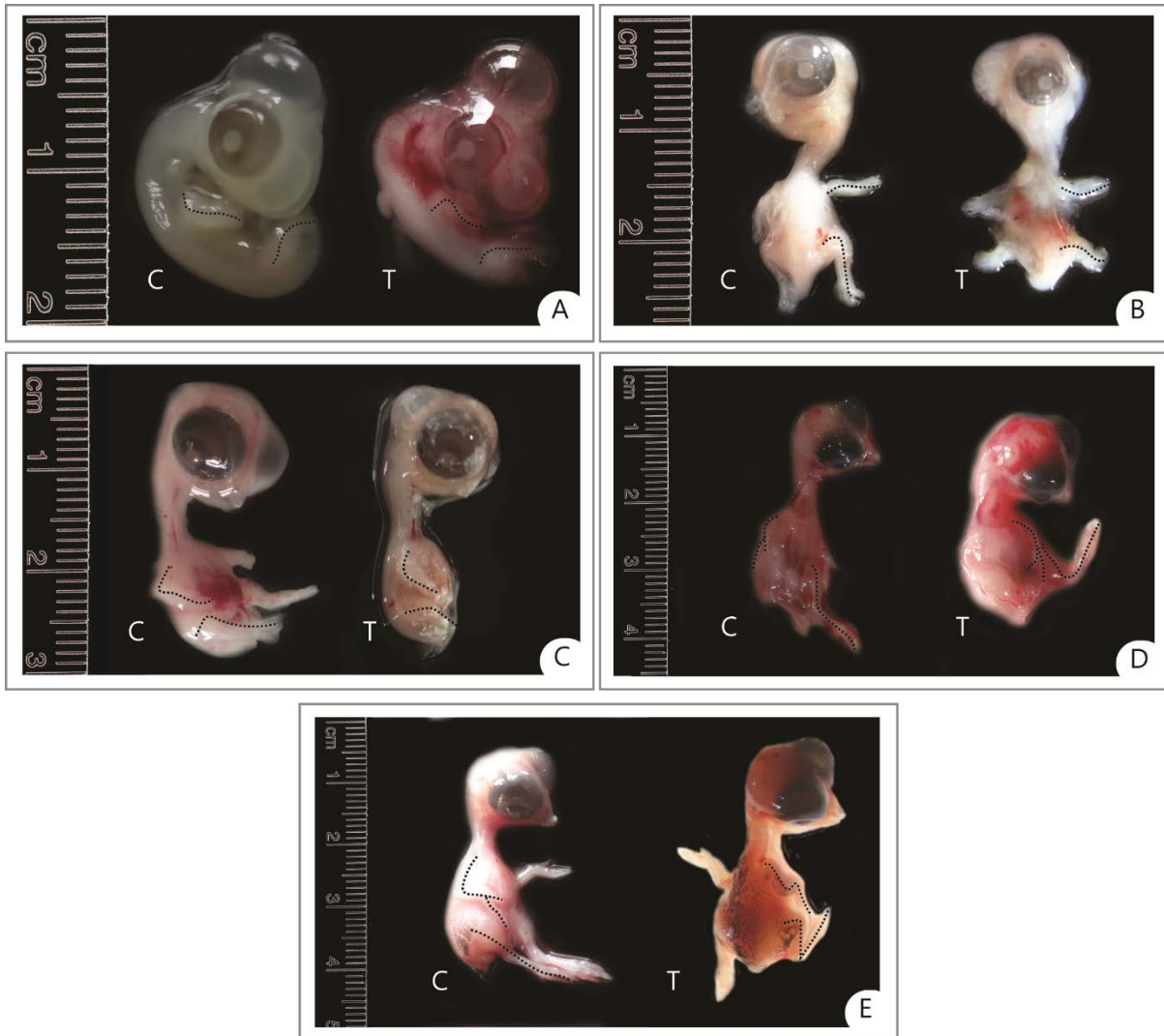


Figure 40: The morphology of limbs in control vs. Treated embryos of day-4 (A), day-6 (B), day-7 (C), day-8 (D), and day-10 (E).control and treated groups are denoted as 'C' and 'T' written inside the figures besides the respective embryos. The limb lengths were marked with black interrupted lines.

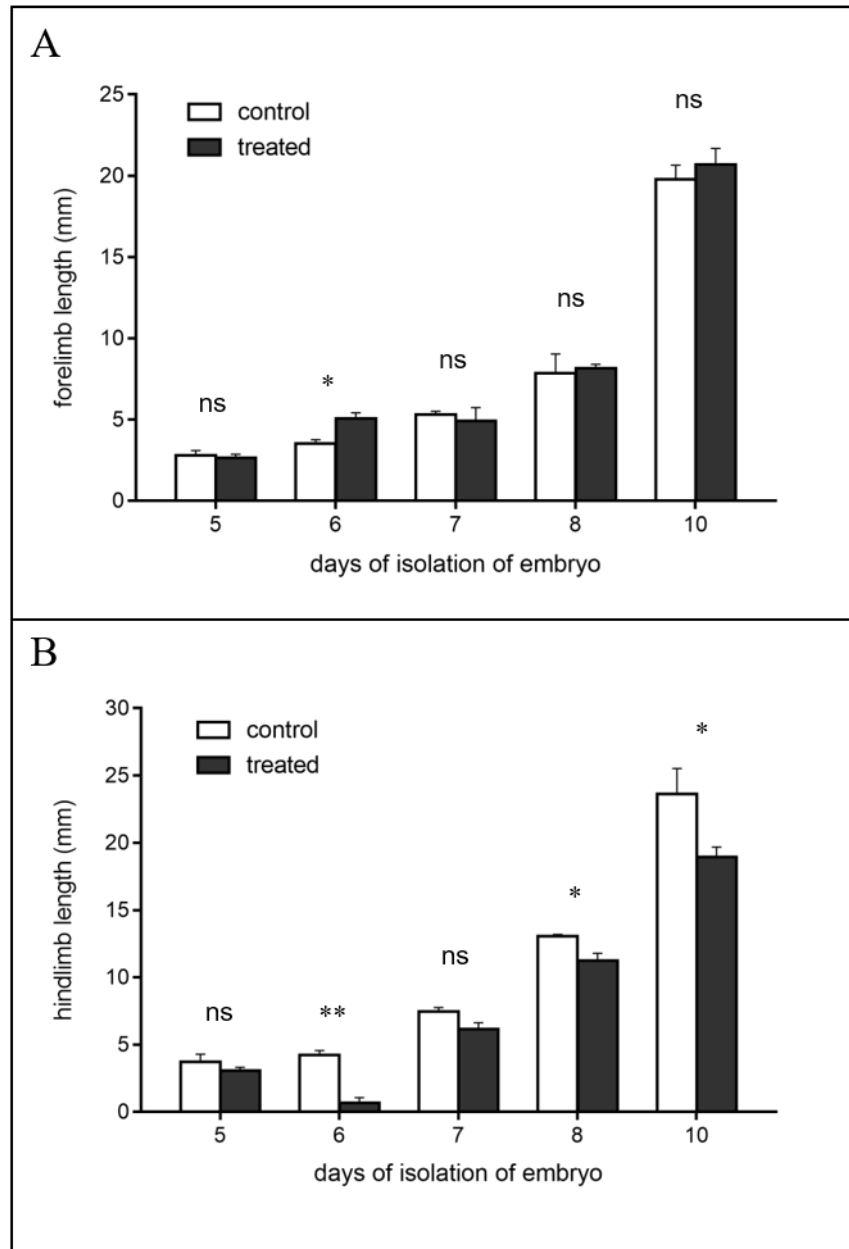


Figure 41: Lengths of control and treated embryonic forelimbs and hindlimbs at various stages of development. Day-6 forelimb was significantly longer than the respective control embryo. Hindlimbs were longer in day-6, 8, and 10 treated embryos as compared to their respective controls.

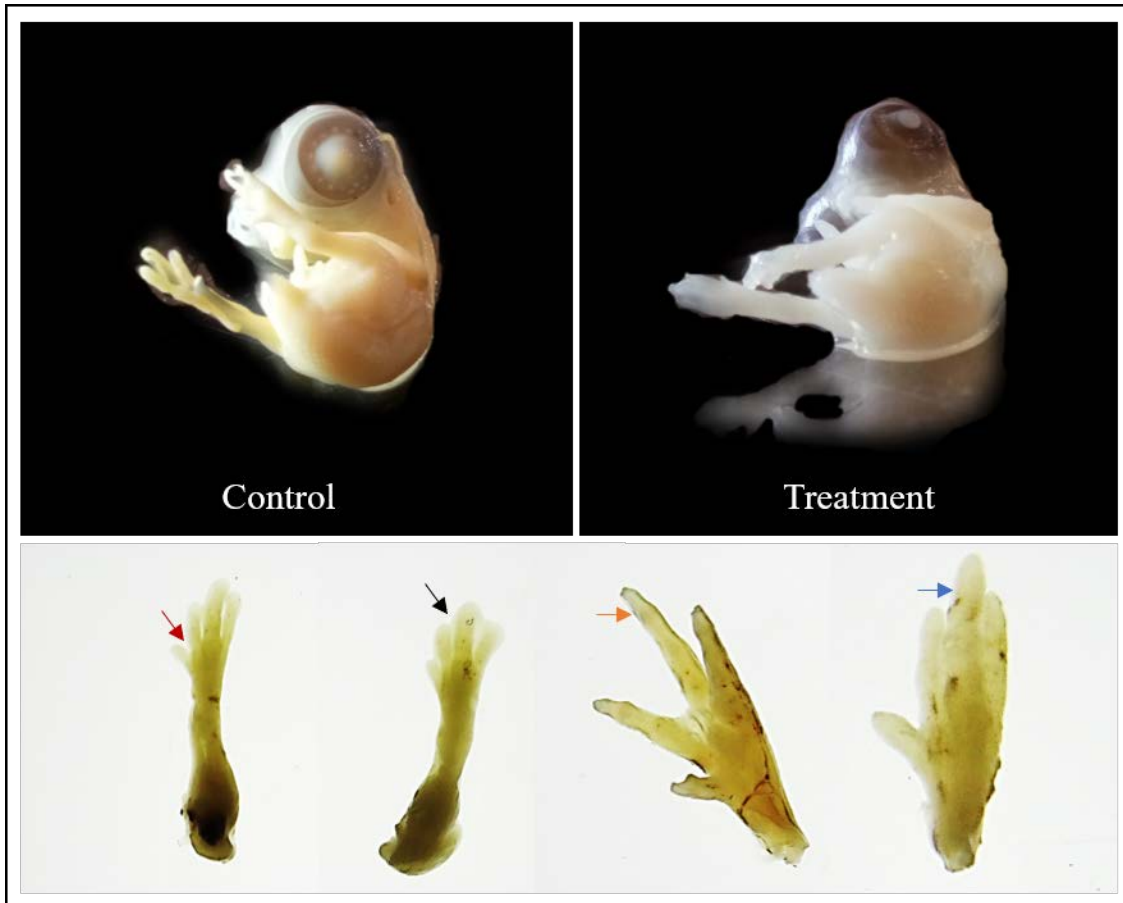


Figure 42: Malformations observed in autopodal regions of experimental embryos as compared to their respective controls. The embryos shown in the figure are day-9 old, with free hindlimb digits in control panel and jointed digits in treatment panel. The image of the lower panel elicits the closer looks of day-8 and day-10 control and treated autopods. The red arrow shows partially digested web at day-8 stage in control embryo, while the black arrow points the presence of web between the digits at the same staged chick embryo. Orange arrow demonstrates the digits completely free of web in the day-10 embryo, while the blue arrow shows the web, still persistent at the edge of digits.

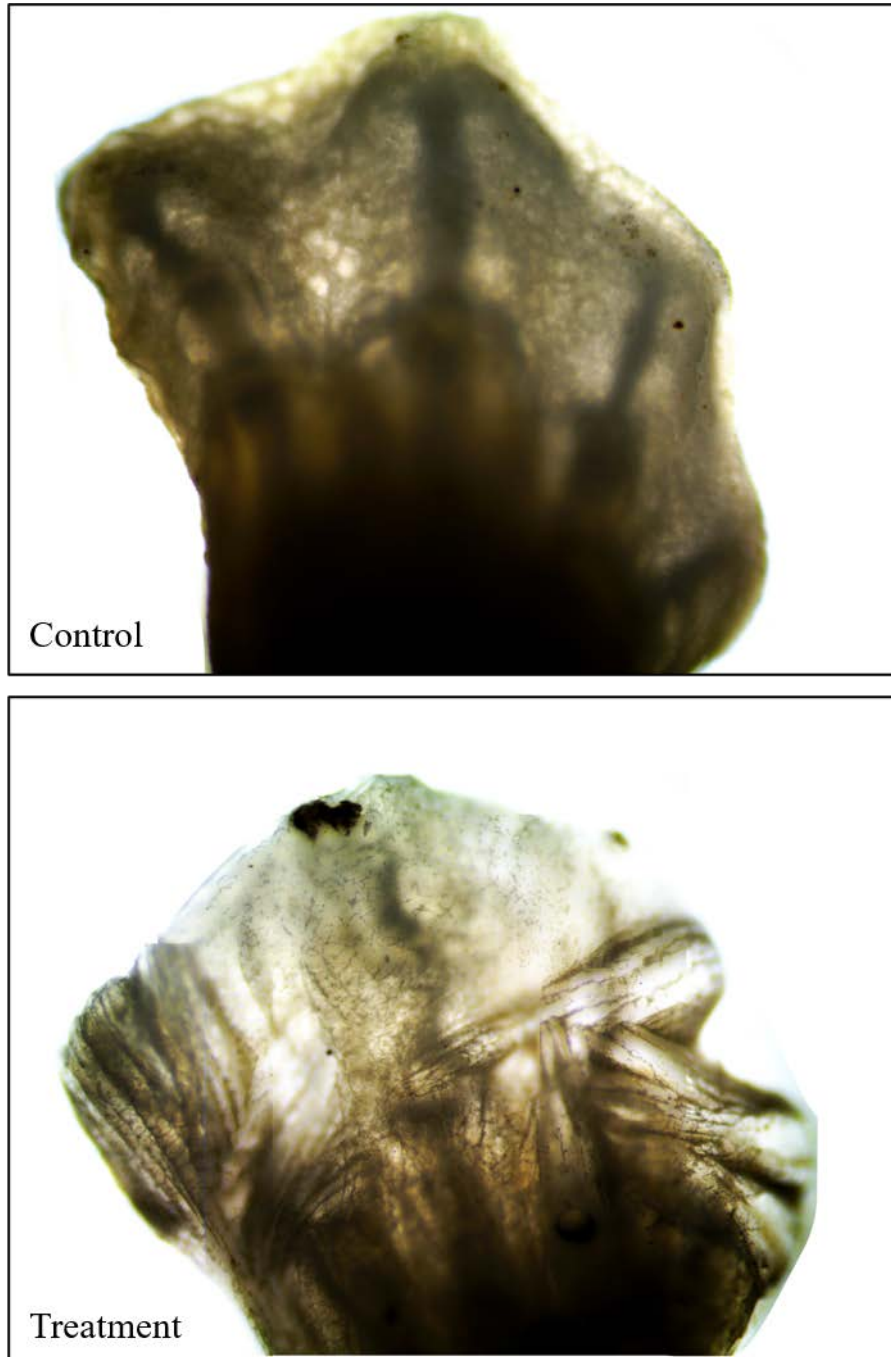


Figure 43: Malformations observed in autopodal regions of day-7 experimental embryo as compared to the control one. The photographs were taken while placing the samples under the phase-contrast inverted biological microscope, to clearly depict the overtly developed skeletal components in the treatment samples as compared to the control ones. The structural components were evidently derailed in case of the treated samples.

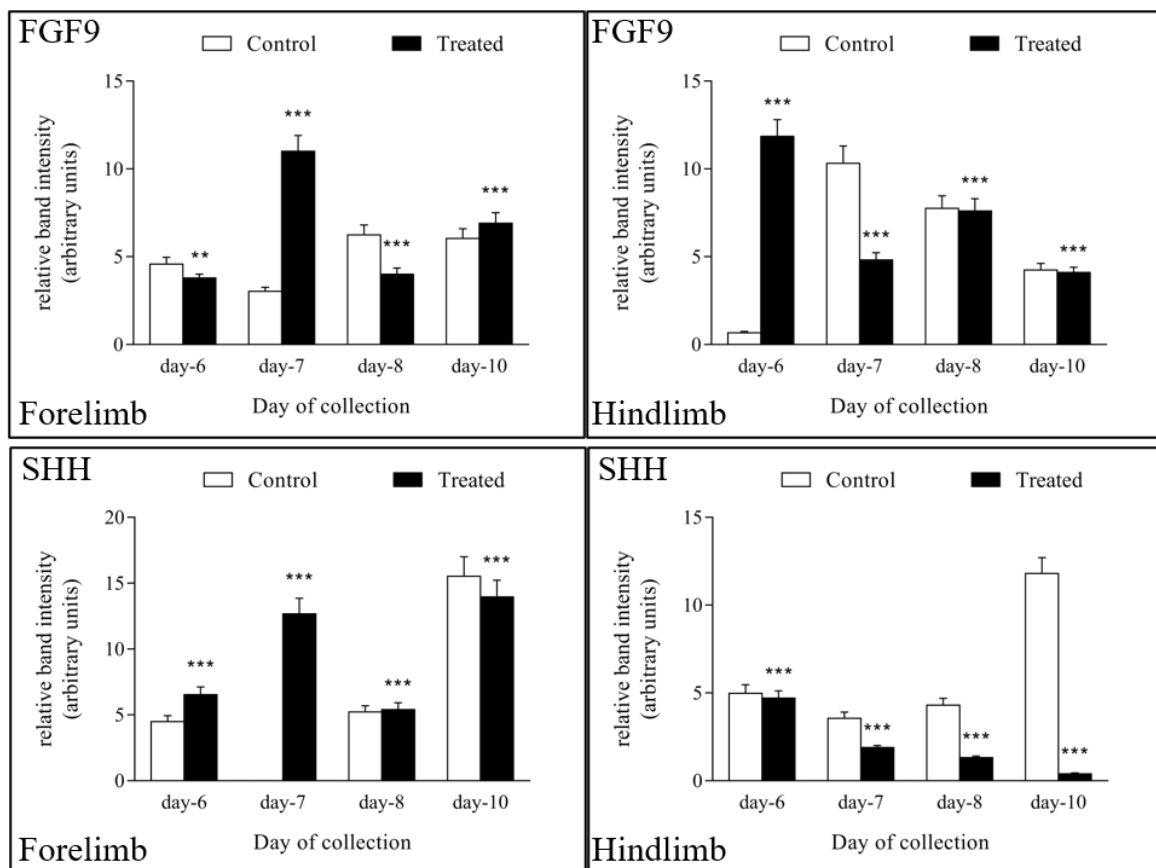


Figure 44: Gene expression pattern of FGF9 and SHH in the embryonic limbs from days 6 to 10. FGF9 significantly dropped at day-6 and day-8, while it increased at day-7 and day-10. The same gene got downregulated in hindlimbs of day-7, 8, and 10, while it got upregulated in day-6 embryos. SHH elevated in embryonic forelimbs from day-6 to day-8, while its level dropped in day-10 forelimbs. On the contrary, it got decreased in all the stages in hindlimbs. *** p value ≤ 0.001 , ** p value ≤ 0.01 , above the plotted values of mean \pm SEM for $n=3$ technical trials from three biological samples each.

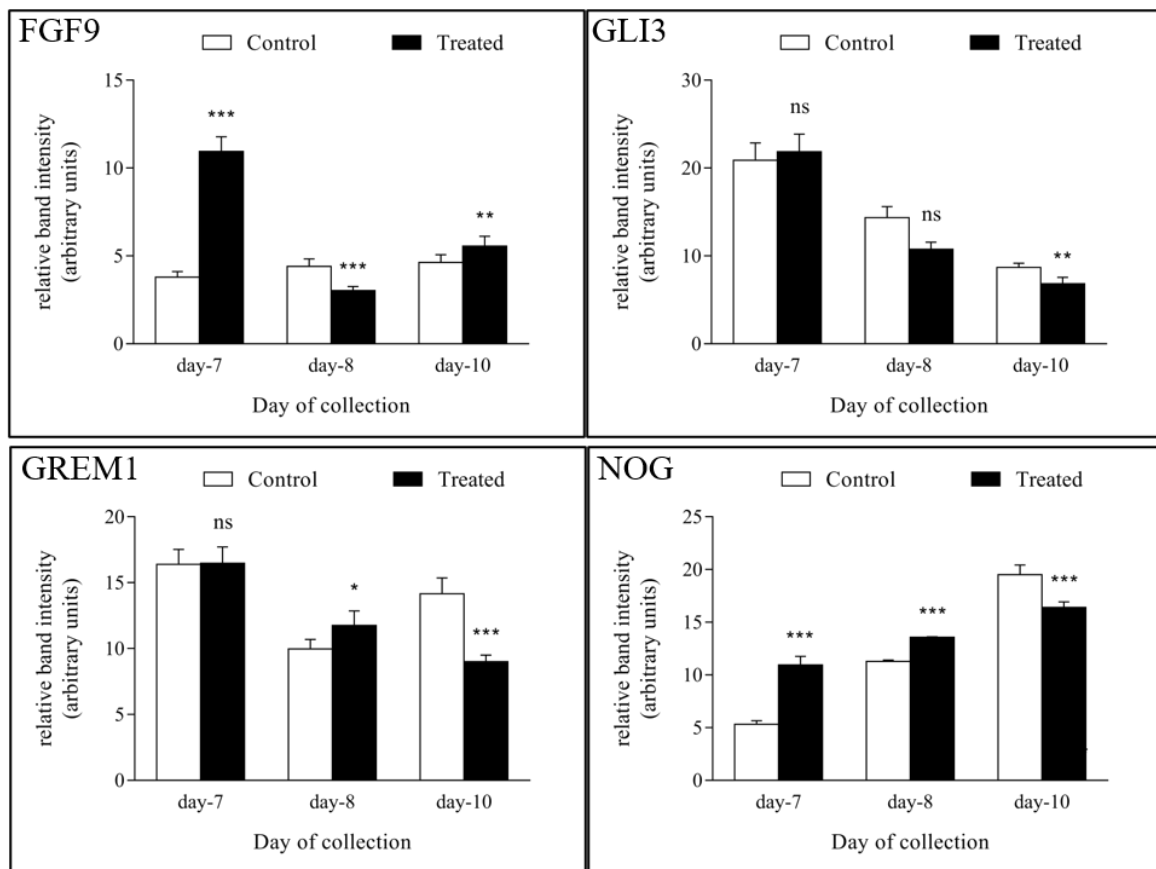


Figure 45A: Gene expression pattern of FGF9, GLI3, GREM1, and NOG in the embryonic hindlimb autopods from days 7 to 10. FGF9 significantly increased at day-7 and day-10, while it dropped at day-8. GLI3 dropped statistically only at day-10. GREM1 increased at day-8 and got alleviated at day-10. NOG increased both on day-7 and day-8, while it was downregulated on day-10. *** p value ≤ 0.001 , ** p value ≤ 0.01 , * $p \leq 0.05$, ns=not significant, above the plotted values of mean \pm SEM for $n=3$ technical trials from three biological samples each.

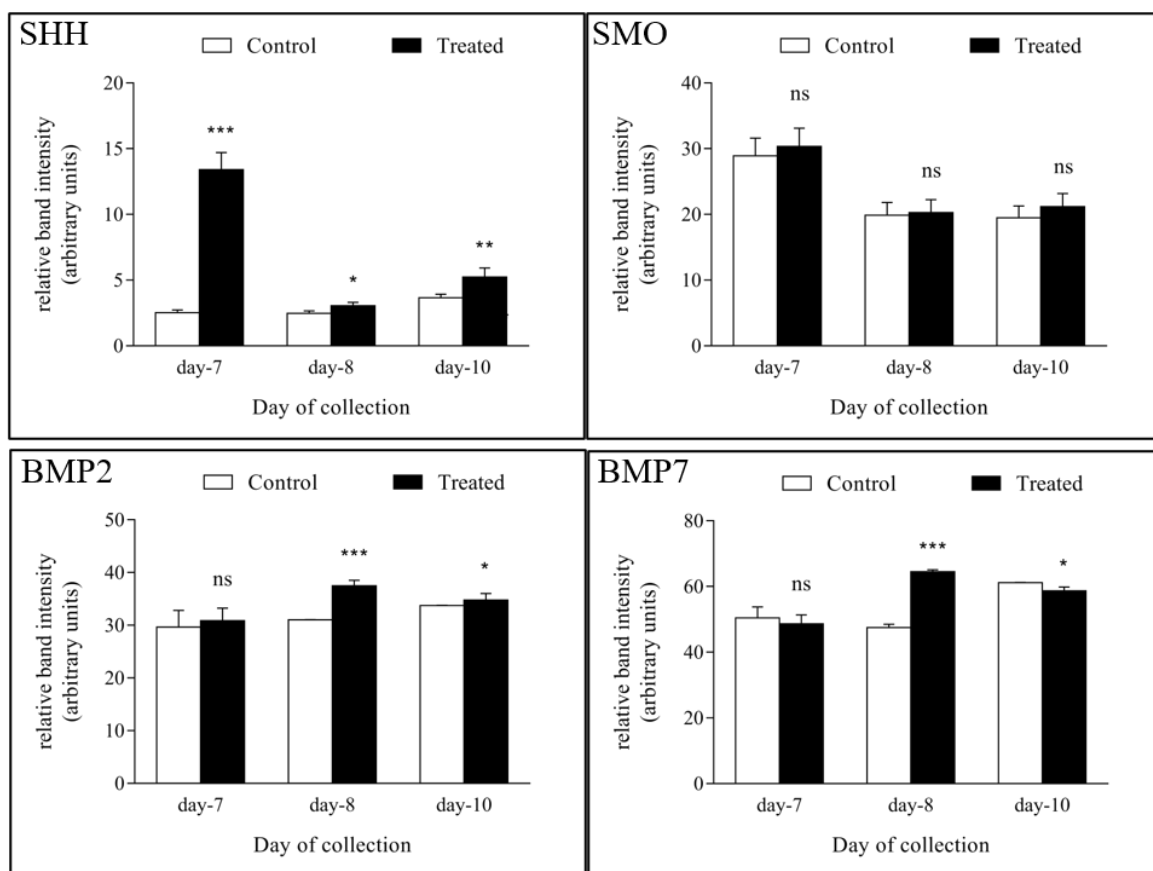


Figure 45B: Gene expression pattern of SHH, SMO, BMP2, and BMP7 in the embryonic hindlimb autopods from days 7 to 10. SHH significantly increased at all the studied stages. SMO did not vary in any of the stages. BMP2 increased significantly at day-8 and day-10. BMP7 increased at day-8 and got alleviated at day-10. *** p value ≤ 0.001 , ** p value ≤ 0.01 , * $p \leq 0.05$, ns=not significant, above the plotted values of mean \pm SEM for $n=3$ technical trials from three biological samples each

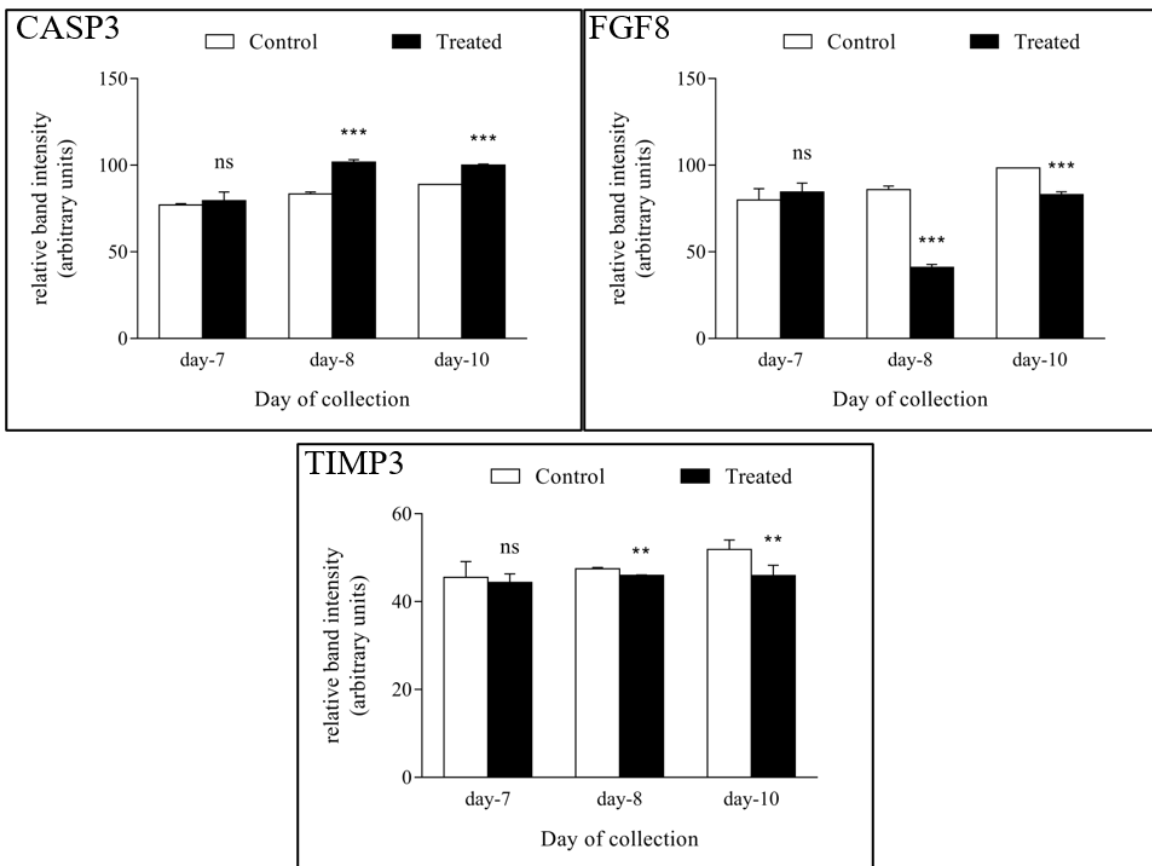


Figure 45C: Gene expression pattern of CASP3, FGF8, and TIMP3 in the embryonic hindlimb autopods from days 7 to 10. CASP3 significantly increased at all the studied stages except for day-7. FGF8 decreased significantly at day-8 and day-10. TIMP3 decreased at day-8 and day-10. *** p value ≤ 0.001 , ** p value ≤ 0.01 , ns=not significant, above the plotted values of mean \pm SEM for $n=3$ technical trials from three biological samples each.

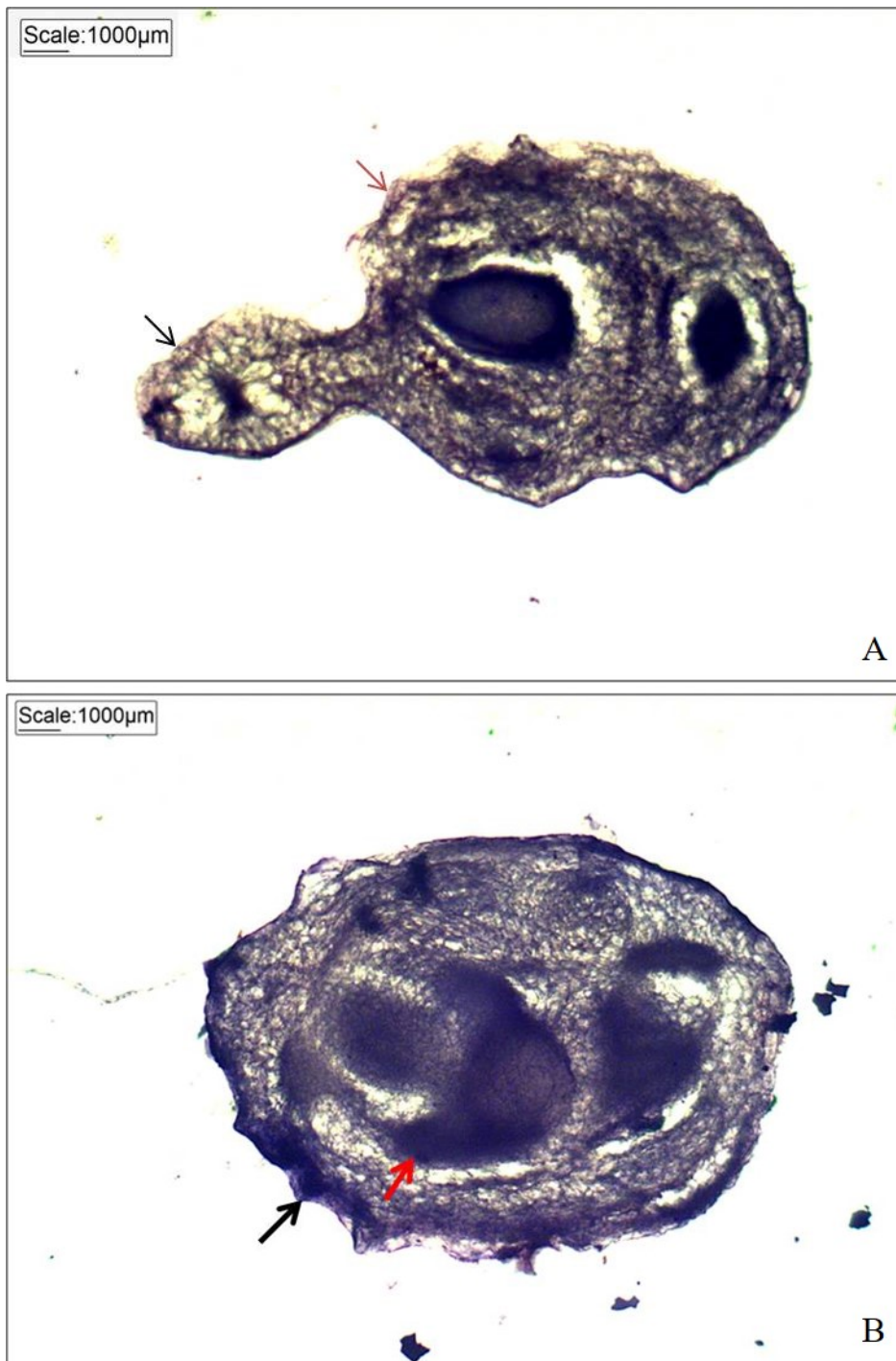


Figure 46: COX-2 immunohistochemistry in day-8 forelimb transverse sections. **A:** forelimb autopod showed presence of it in epithelial layer (black arrow), developing wing membrane region (red arrow). **B:** stylopod-zeugopod junction image shows presence of COX-2 in wing membrane (arrow).



Figure 47: COX-2 immunohistochemistry in day-8 hindlimb transverse sections. **A:** zeugopod junction image shows presence of COX-2 in wing membrane (white arrow). **B:** hindlimb autopod showed presence of it in epithelial layer (black arrow).

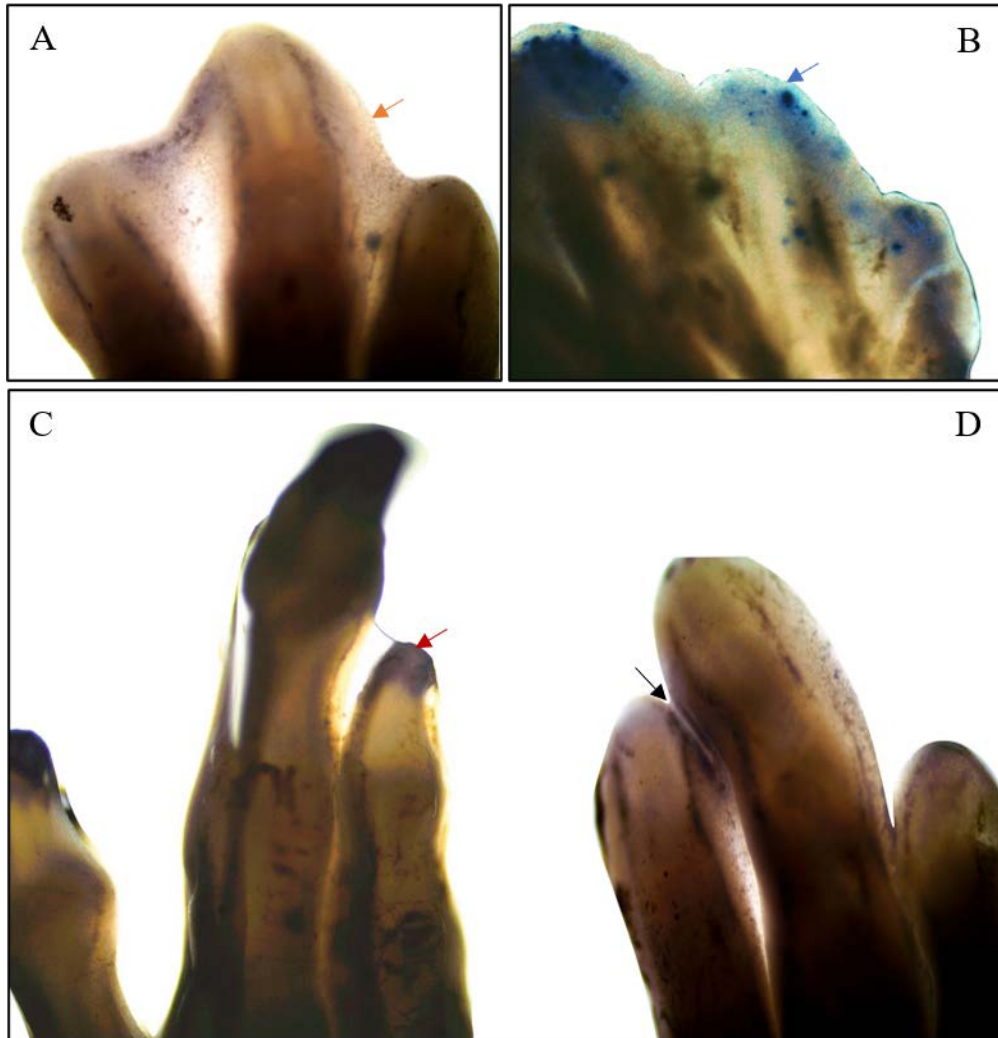


Figure 48: *cl. Caspase3* immunolocalization in day-8 and day-10. **A:** control hindlimb autopod showed presence of *cl. Caspase3* in the outer edge of web fading towards interdigital zone (red arrow). **B:** Presence of *cl. Caspase3* was marked in the wavy edge of treated hindlimb web (blue arrow). **C:** The distal end of digits showed presence of *cl. Caspase3* (red arrow) in the control day-10 embryo. **D:** *cl. Caspase3* was localized in the interdigital area along with the distal end (black arrow) of treated embryonic hindlimb autopod.

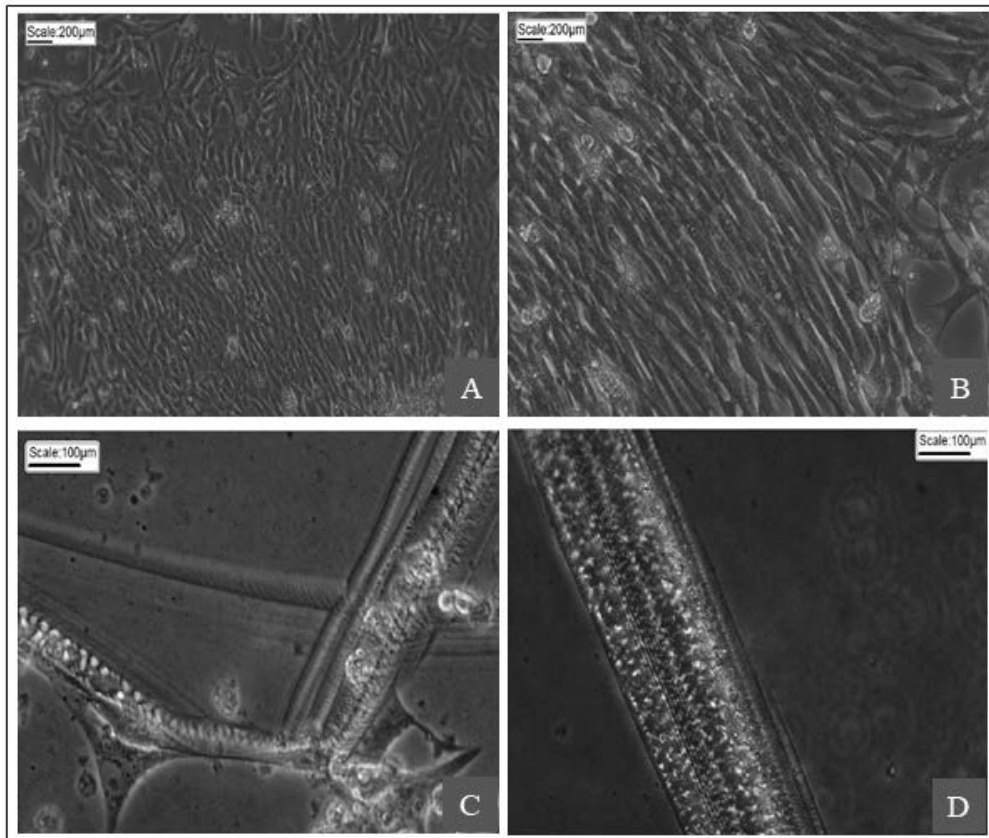


Figure 49: Control morphology of cultured chicken embryonic skeletal muscle cells. A: A typical fibroblastic morphology of substratum-anchored cells seen in phase-contrast microscopy based 100X field view (day 1), scale: 200 μm ; B: Myogenic cells fusing for formation of primary myotubes (day 4), scale: 200 μm ; C: Differentiating cells forming secondary myofibres (day 10), scale: 100 μm ; D: Morphology of myofibre in control culture, scale: 100 μm

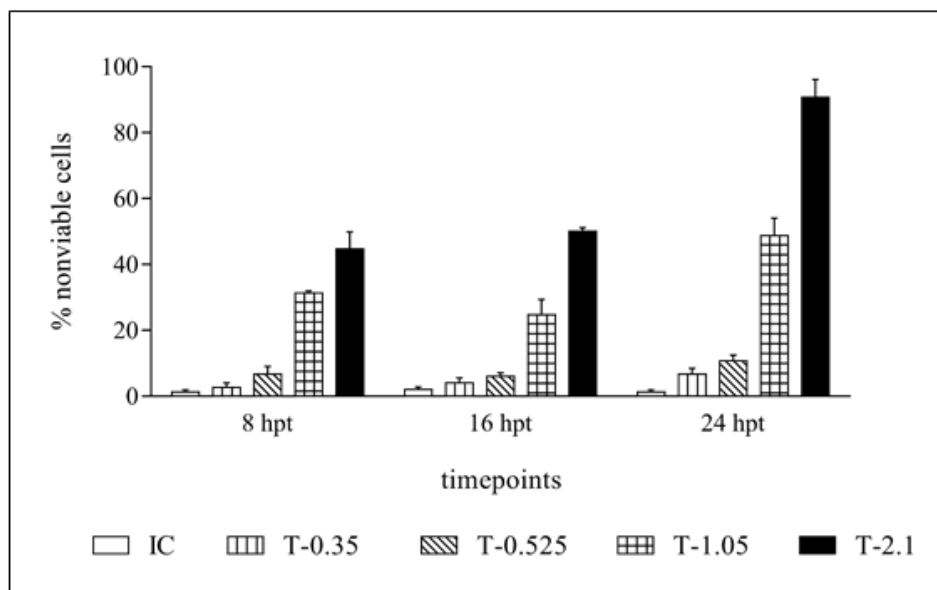


Figure 50: Trypan blue cell exclusion test. Treatment of 0.35 ppb anti- α -DG did not cause any significant loss of viability until 24 hours of treatment. 2.1 ppb caused excessive mortality, while dose of 1.05 ppb did not show stable increase in non-viability with passing time. Treatment with 0.525 ppb anti- α -DG caused stable time-dependent impact on cell viability rather than rapid or sluggish effect of other concentrations, and was finalised as dose for other experiments. hpt=hours post treatment.

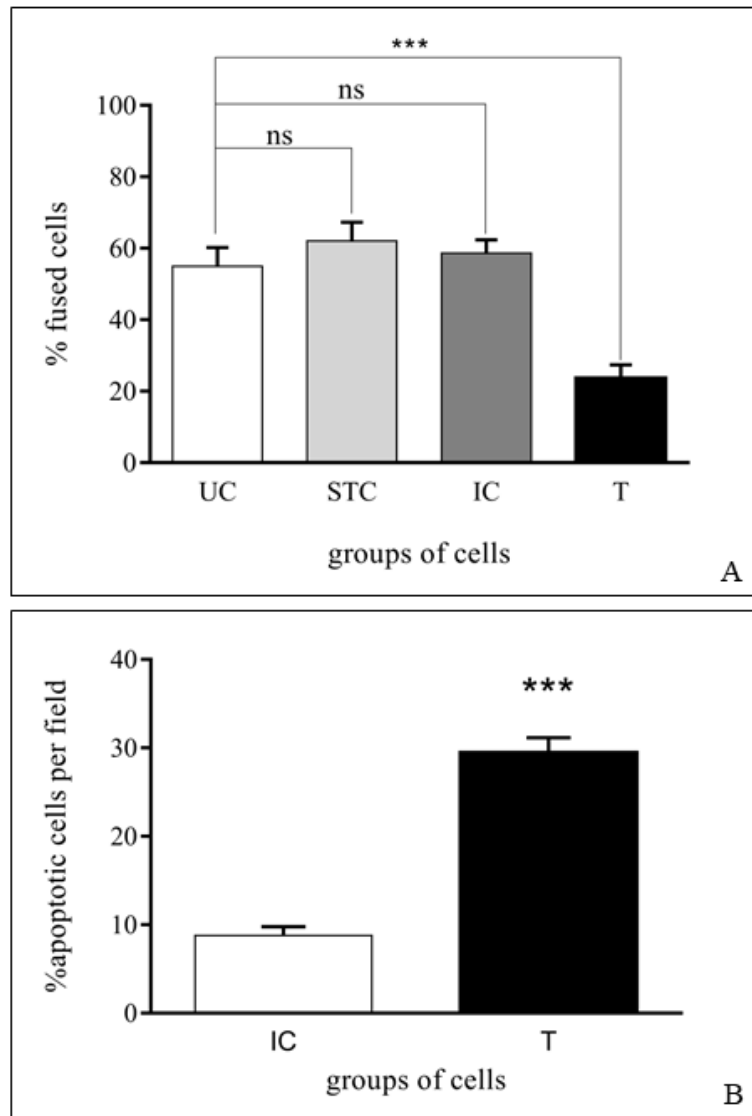


Figure 51: Fusion index and apoptotic index. fusion index was calculated for various controls, namely untreated control (UC), supernatant treated control (STC), and isotype control (IC), as well as for treatment (T) cultures. Fusion index dropped to half its control level in case of treatment culture. Apoptotic index was only calculated for IC and T groups as there was no variation in other characteristics of all the control groups. It was found that anti- α -DG treated cells showed increased apoptosis as compared to control group.

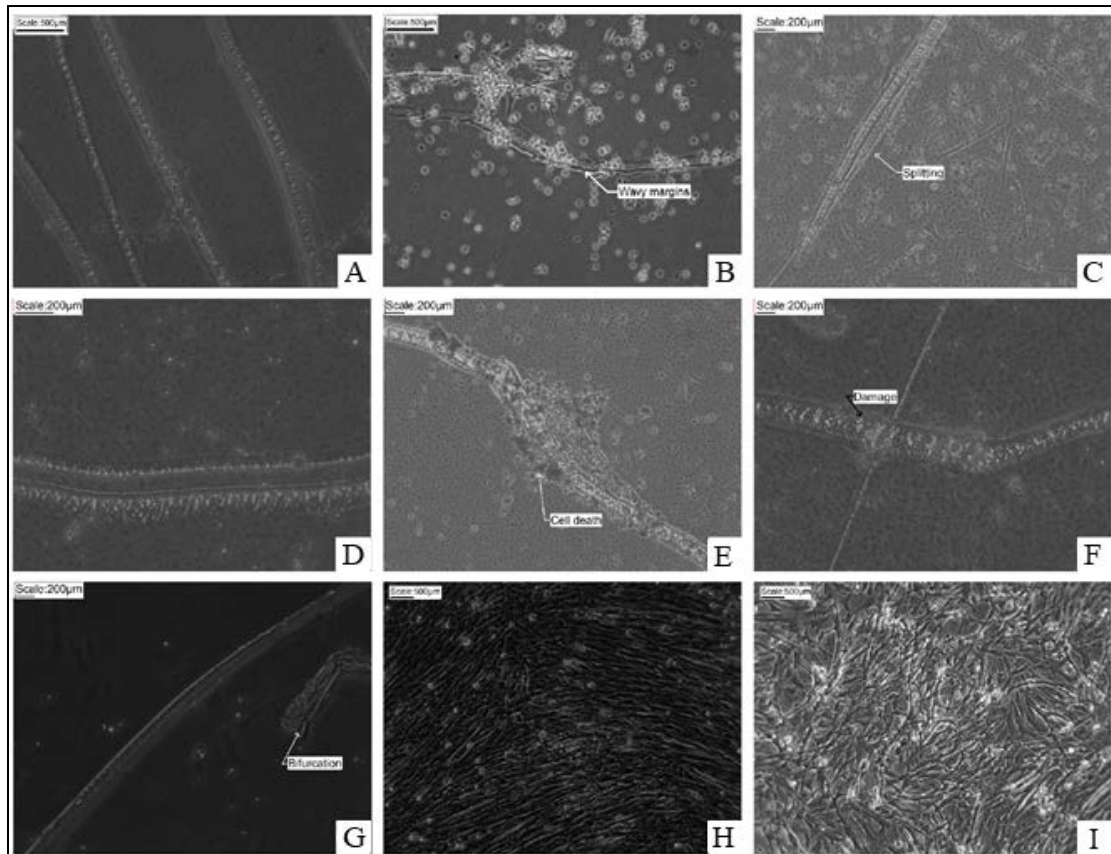


Figure 52: Morphological features of IC and T cultures. (A) Control morphology at $\times 400$ magnification, scale $100\ \mu\text{m}$. (B) Wavy margins of myotubes formed in treated culture, scale $200\ \mu\text{m}$. (C) Central splitting in developed myofibre of treated culture, scale $200\ \mu\text{m}$. (D) Disruption along sarcolemma of myofibre in treated culture, scale $200\ \mu\text{m}$. (E) Cell death in treated myotube, scale $200\ \mu\text{m}$. (F) Myofibre damaged along its length in treatment group, scale $200\ \mu\text{m}$. (G) Treated myofibre end-splitting, scale $200\ \mu\text{m}$. (H) IC group cells showing normal morphology of myotubes growing in a unidirectional manner, scale $200\ \mu\text{m}$. (I) Treated myotubes growing in various directions unlike normal growth, scale $200\ \mu\text{m}$.

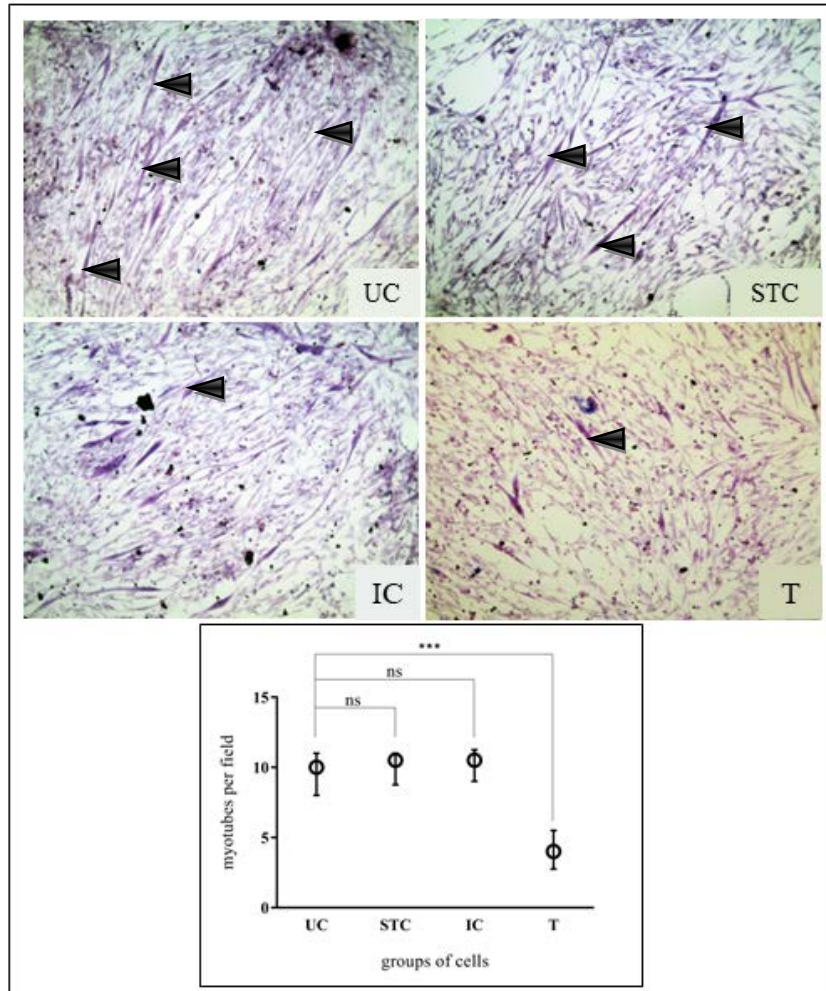


Figure 53: Variation in myotube numbers. Black arrowheads point at the myotube in each of the images. (A) $\times 100$ field view of UC group with numerous myotubes stained with LADD for ease of evaluation. (B) Representative view from one of the culture vessels treated with supernatant of anti- α -DG (STC group) showing number of myotubes per view. (C) Cells of IC group showing abundant myotubes. (D) Remarkable reduction in numbers of myotubes in treated cells. Graph: The values when analysed by performing one-way ANOVA showed that only treated cells had significantly less numbers of myotubes per field. There was no significant difference among all the control groups. *** $p \leq 0.001$.

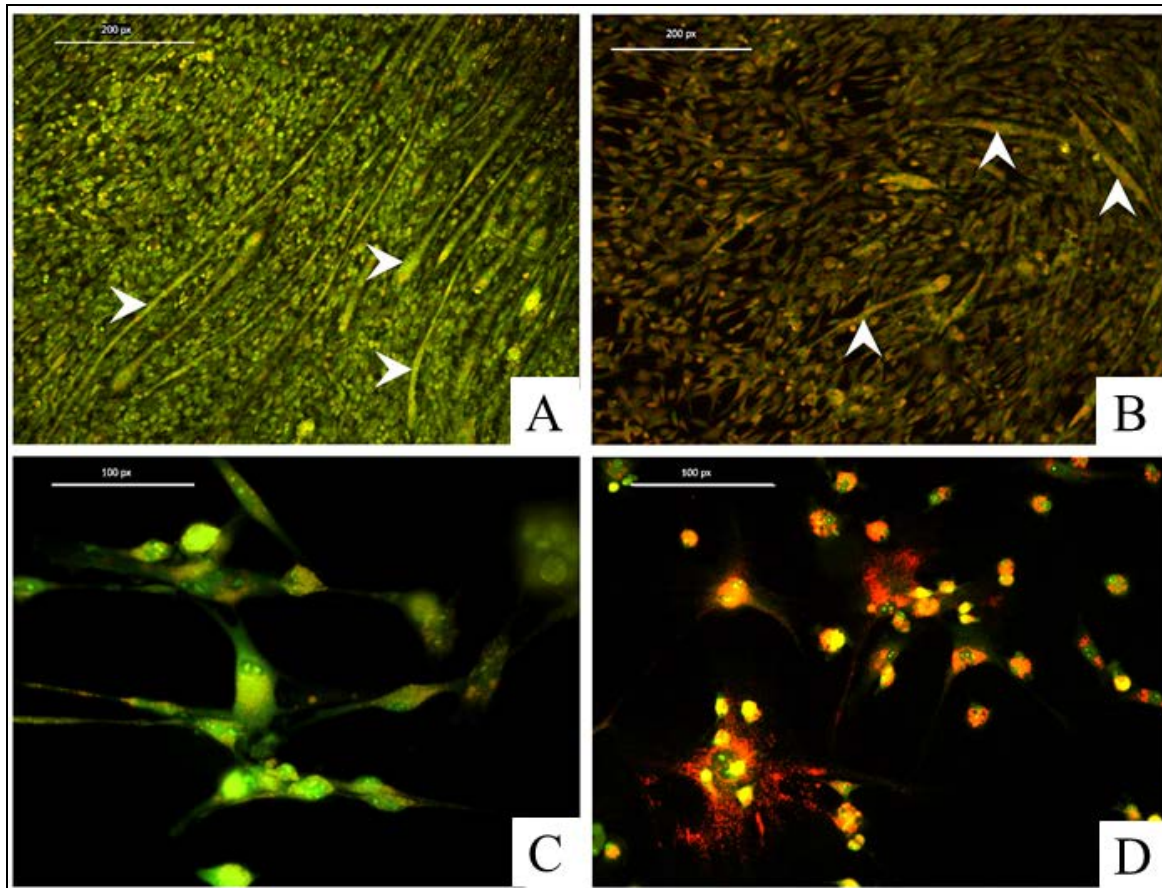


Figure 54: EtBr/AO staining in IC vs. T cells. **A** and **C** show control cells with minimum amount of apoptotic orange fluorescence and maximum amount of viable green phenotype. **B** and **D** show higher number of cells exhibiting apoptotic and necrotic phenotype. First and second row of images are 200x and 400x field views respectively. White arrow heads specifically mark the myotubes in normal (**A**) and apoptotic (**B**) states.

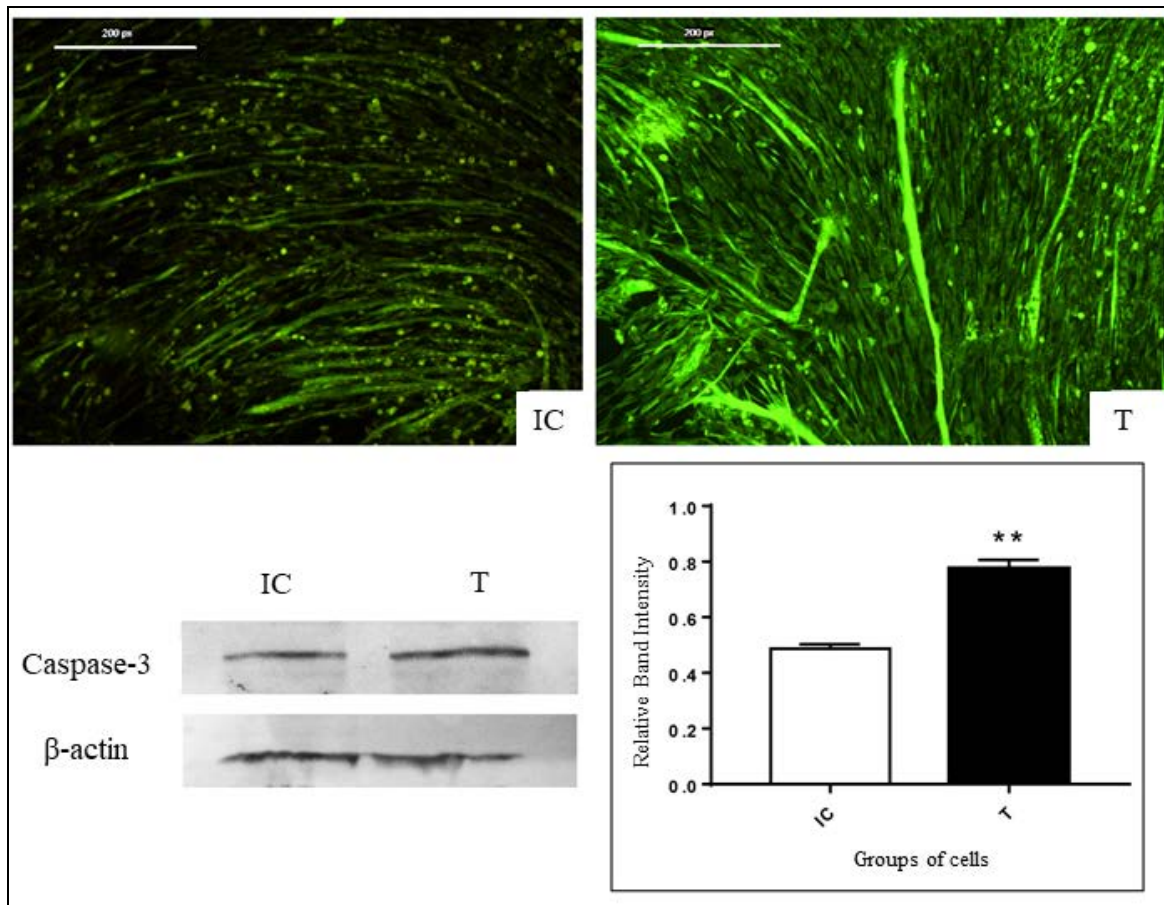


Figure 55: Immunolocalization of cleaved Caspase-3 in control and treated cells. The treated (anti- α -DG) myotubes intensively stained with cleaved Caspase-3 antibodies when compared to control myotubes. 100x field view, scale: 200 px. Western blots of cleaved Caspase-3 relative to the internal control β -actin showed significant increase of cleaved Caspase-3 in treated cells when compared to control. $** p \leq 0.01$.

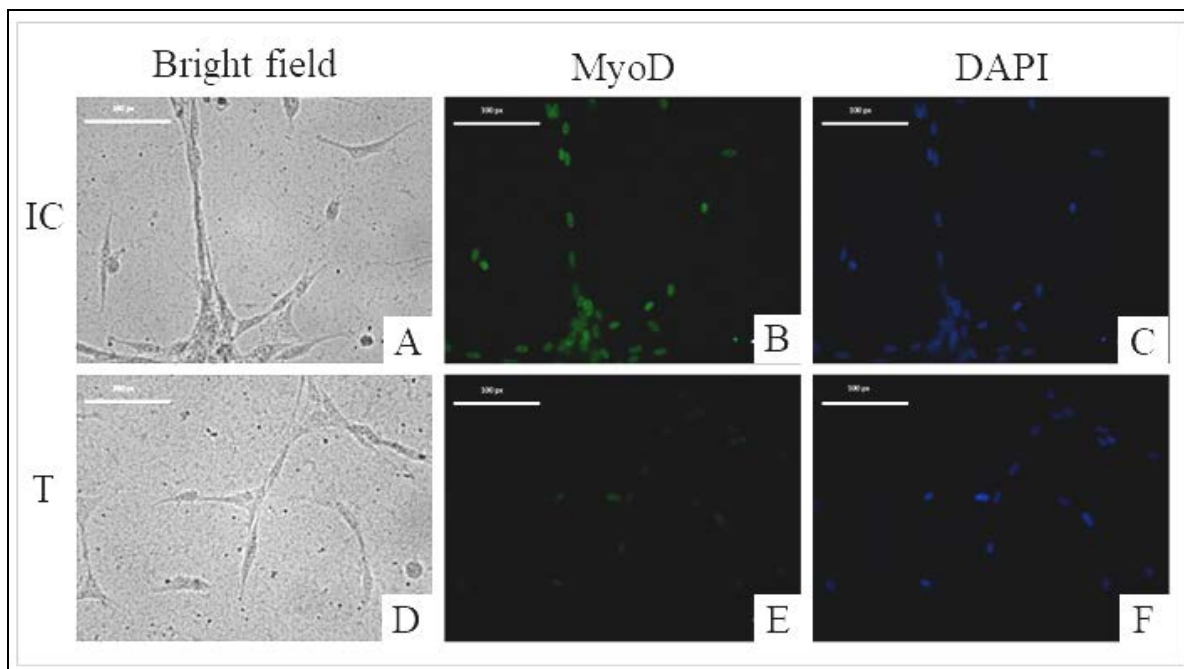


Figure 56: Immunolocalization of MyoD1 protein in IC vs. T group. The upper panel (A, B and C) shows the control cells stained brightly with MyoD antibodies. The lower panel comprising of D, E and F show treatment (anti- α -DG) group cells wherein, very few cells have got immunostained with MyoD antibody. 400x field view, scale: 100 px for each image.

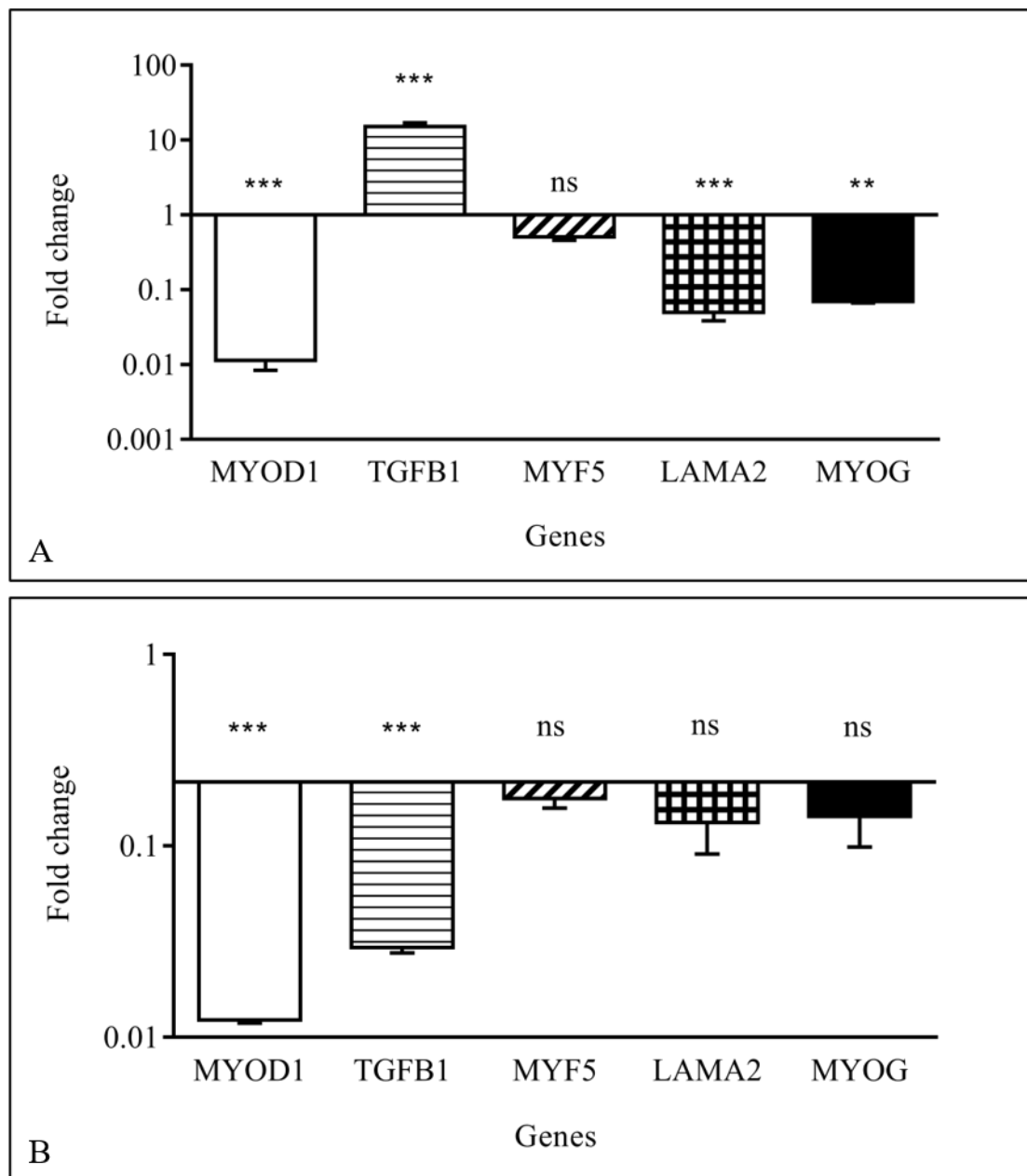


Figure 57: Quantitative difference in gene expression pattern. ** $p \leq 0.01$, *** $p \leq 0.001$. **A:** expression of myogenic genes dropped in anti- α -DG treated cells as compared to IC cells. $TGF\beta 1$ (inflammatory gene) increased in the treated group as compared to control. **B:** $TGF\beta 1$ expression dropped in the etoricoxib treated group as compared to dystrophic cells (anti- α -DG treated cells), along with a significant downfall of MYOD gene.

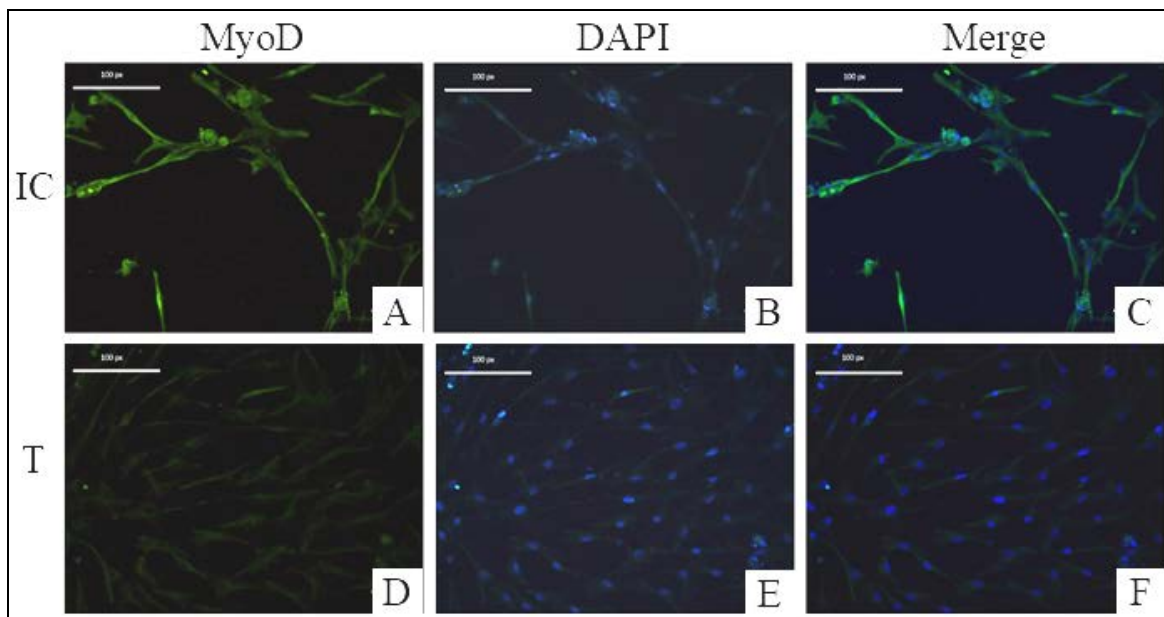


Figure 58: *MyoD* immunocytochemistry. Etoricoxib treatment (T) decreased *MyoD* concentration as compared to the IC cells, resembling to the case of anti- α -DG treated cells, showing lack of rescue of *MyoD* levels by etoricoxib.